CHAPTER 4

Water Relations of Forest Fuels

RALPH M. NELSON, JR.
USDA Forest Service, Rocky Mountain Research Station, Fire Sciences Laboratory, Missoula, Montana

I. INTRODUCTION

Earlier chapters have described forest fire behavior and effects, the general nature of forest fire flames, and the processes of combustion and smoke production in forest fuels. It was pointed out that moisture in these fuels acts to retard the rate of combustion. Among the fire behavior factors affected are the preheating and ignition of unburned fuels, rate of fire spread (or fire growth), rate of energy release, and production of smoke by burning and smoldering fuel. If we are to improve our understanding of these and other aspects of fire behavior, we must be able to quantify fuel moisture content within reasonable bounds. Moisture content, expressed as a fraction, is the mass of water held by unit mass

of ovendry fuel and is determined primarily by fuel type and weather. It also may be expressed as a percentage of the fuel ovendry weight by multiplying by 100%.

For our purposes, fuels will be considered as living or dead and, within these broad categories, as individual particles or a collection of particles making up a fuel complex, or stratum. In many cases, of course, a fuel complex is composed of a mixture of live and dead particles from various fuel types whose moisture contents may vary over a wide range. The open grasslands of the southwestern United States exemplify a single fuel stratum, whereas the palmetto-gallberry-southern pine fuels of northern Florida exhibit at least three strata—a mat of pine needles in varying stages of decay intermixed with various living grasses and forbs, an intermediate layer of shrubs, and a pine overstory. The trunks of standing individual trees greater than 5–10 cm in diameter usually are scorched or charred by fire but do not burn and are not considered part of the fuel complex. In the conifer forests of the western United States and Canada, needle ladders (sometimes referred to as needle drape) often extend from the canopy to the ground so that fire can climb into the tree crowns. Similar behavior in some other conifer species such as spruce is caused by branches extending to the ground. When the crown fuels are drier than normal and winds are strong, these transitions from surface fire to crown fire occur with a large increase in energy release rate. The fire appears to acquire a violent character, and its increased energy often renders useless any attempt to control it.

The present chapter begins with a review of the influence of moisture on the combustion of forest fuels and how fuel characteristics determine the moisture content level of these fuels. It summarizes current understanding of the amount of water these fuels can hold, gain and loss of this water, and how the governing processes have been described mathematically. Only fuels associated with or originating from vascular plants (grasses, shrubs, and trees as opposed to mosses and worts that lack internal structure for transporting water) are considered. The discussion of live fuels emphasizes the physiological aspects of water transfer, but only a few studies related to mechanisms of water transport in these fuels are discussed. For example, the effects of photosynthesis, respiration, and growth on water potential and water movement are not described. Brief mention is made of soil water transport which, itself, has been a prominent topic in many soil physics and hydrology texts. In the case of dead fuels, a description of what the author believes are the more relevant studies is given. Only a few of the published studies of moisture content change in wood and forest fuels have dealt with diurnal change; a glimpse at prediction models for diurnal moisture variation is provided. Near the end of the chapter, several methods of measuring the moisture content of live and dead forest fuels are briefly discussed, and the reader is referred to works related to the fuel moisture aspects of current fire behavior and fire danger rating systems. Information on the general topic of forest fuel moisture relationships may be found in Luke and McArthur (1978), Chandler *et al.* (1983), Pyne (1984), and Pyne *et al.* (1996).

II. FOREST FUELS

The behavior of a spreading fire is determined by factors such as weather, topography, fuel quantity, and fuel moisture content. In practice, the burning characteristics of individual forest and wildland fuel particles are difficult to describe, but the influence of moisture content, particle physical properties, and particle arrangement on the burning characteristics of vegetation layers or litter and duff is even more complex and not well understood. This section discusses the effects of fuel moisture content on fuel burning rates and the fuel characteristics related to moisture content change.

A. Fuel Classification

Because forest fires usually are categorized according to the location of the uppermost fuel stratum through which they burn (ground, surface, or crown fires), it makes sense to think of fuel classification in the same way. Thus fuels may be classified as ground fuels, surface fuels, or crown fuels. Ground fuels consist of the highly decomposed organic material in contact with the inorganic layer and include duff, roots, peat, and rotten wood or bark coming from downed twigs and branches. Next to the ground fuel is a layer of surface fuels consisting of recently fallen and partially decomposed tree leaves (and/or conifer needles), fallen twigs, bark and branches, live or dead grasses, forbs, and shrubs less than 1.8 m tall (Davis, 1959). In moist climates, the fuels above mineral soil have three components: the recently cast *litter layer,* the partially decomposed *fermentation layer,* and the well-decomposed *humus layer.* Stocks (1970) refers to duff as all material above the upper surface of the mineral soil. A distinction between litter and duff is made in this chapter, however, with "litter" referring to the litter and fermentation layers and "duff" referring to the humus layer. The characteristics of duff layers are discussed further in Chapter 13 in this book. Dead ground and surface fuels contain both free and bound liquid water and are sensitive to precipitation and to changes in atmospheric relative humidity and temperature. Crown fuels include the canopies of most conifers and the chaparral and pocosin shrub types typical of the southwestern and southeastern United States. The latter two fuel types, which some investigators would categorize as surface fuels, grow to a height of 5 m or more. The moisture content of these live fuels is determined primarily by environmental and physiological factors. The canopies of deciduous species also are crown fuels, but fires rarely spread through these strata because the crowns are relatively sparse and have higher moisture contents than conifers. Exceptions occur under dry, windy conditions and when the fuels contain highly volatile and flammable substances, as in various species of *Eucalyptus.*

B. Fuel Burning Rates and Moisture Content

The effect of fuel moisture on fire behavior is to slow the rate of burning, or rate of fuel consumption. For a spreading line of fire, the average burning rate can be computed from the mass of fuel consumed per unit area of ground divided by the time required to consume fuel on the area. Thus high fuel moisture content retards the rate of fuel consumption per unit of burning area (kg m^{-2} s^{-1}) by decreasing the mass of fuel consumed and increasing the particle burning time, or *particle residence time* (the time during which flame resides on individual particles in the fuel layer combustion zone). In addition, it increases the fuel preheating time. With respect to the thermal history of unit mass of fuel, the various phases of combustion include the processes of preheating, volatilization, charring, smoldering, and glowing; these are described in Chapters 3 and 13 in this book.

Consider first the fuel preheating time (or ignition time). The heat required for the onset and completion of volatilization of the fuel (volatilization begins at about 200°C and is assumed complete when the fuel temperature reaches 400°C) is called the heat of ignition Q_T (kJ kg^{-1}) by Wilson (1990) and is computed from the defining equation

$$Q_T = Q_f + MQ_M \tag{1}$$

where Q_f (kJ kg^{-1}) is the heat required to raise unit mass of dry fuel from ambient temperature to 400°C, Q_M (kJ kg^{-1}) is the energy to heat unit mass of water to 100°C and then vaporize it, and M is the fractional moisture content (a fuel particle or layer average expressed on an ovendry weight basis). Thus, an increase in M increases the amount of heat required to raise the temperature of unit mass of fuel from ambient temperature to 200°C and increases the preheating time. Various investigators have observed increases in ignition time with increasing M in dead and live fuels (Fons, 1950; Xanthopoulos and Wakimoto, 1993). The analytical studies of Albini and Reinhardt (1995) suggest that the increase in ignition time is due to increases in particle thermal conductivity and volumetric heat capacity with increasing M. A different aspect of ignition deals with what happens when firebrands, either short or long range, are blown or dropped into unburned fuels. Again, preheating and ignition are slowed by fuel moisture content, and the heat demand may be estimated by Eq. (1). Blackmarr (1972) has shown that the probability of ignition in slash pine litter is a strong function of moisture content and firebrand characteristics.

A second effect of fuel moisture on the burning rate involves a decrease in fuel consumption owing to the interaction among various fire behavior characteristics. The available fuel loading, defined here as the mass of fuel consumed

per unit area of ground during flaming combustion, depends in a complicated way on moisture content, flame temperature, and the mass fractions of volatiles and char produced during combustion of unit mass of original fuel. The fuel chemical composition and rate of thermal decomposition are two factors affecting the relative amounts of volatiles and char produced which, in turn, determine the heat of combustion and the fraction of fuel available for flaming combustion. These relationships are discussed in detail by Albini (1980) and Susott (1982). The presence of moisture also causes a reduction in flame temperature because some of the heat generated in combustion is used to heat the inert water vapor in the products of combustion and because oxygen in the air is diluted by water vapor leaving the heated fuel (Byram, 1959). The reduced temperature retards the rate of decomposition and tends to drive the combustion process toward production of char rather than toward production of high-temperature volatiles. Results from burns of *Eucalyptus* leaves in a flow calorimeter (Pompe and Vines, 1966) suggest that water in fuel promotes smoke formation, reduces the heat of combustion, lowers the rate of temperature rise of air flowing in the calorimeter, and leads to much less intense burns. The effect of moisture on fuel consumption was estimated by Van Wagner (1972a) who used data from experimental fires spreading in jack pine, red pine, and white pine stands to develop a semiempirical relationship showing that duff consumption decreases as M increases. His equation for the weight of duff consumed, $W\,(\mathrm{kg\,m^{-2}})$, is given by

$$W = 0.941(1.418 - M)/(0.1774 + M) \tag{2}$$

suggesting that consumption in these fuels approaches zero when M approaches 1.418. The origin of Eq. (2) is discussed in Chapter 13 in this book. In this model, downward transfer of heat by radiation in the fuel layer combustion zone drives off moisture and then raises the temperature of the dry duff to the ignition point. Closure of the model requires a decrease in the emissivity of the flaming front with increasing M, suggesting that reduced radiative transfer to unburned fuel constitutes yet another means of slowing the rate of fuel consumption. King (1973) discusses the reduction of flame emissivity due to presence of moisture in terms of a reduction in soot concentration and an increase in carbon monoxide concentration according to the water gas reaction in which water vapor and carbon (soot) combine to form carbon monoxide and hydrogen.

The third effect of fuel moisture on the rate of burning is an increase in the fuel particle residence time. Albini and Reinhardt (1995) have shown with experimental and theoretical studies that, to the extent that flaming combustion is fueled by a simple sublimation process, the characteristic particle burning time is proportional to Q_T from Eq. (1). Because this demand for heat is satisfied

by radiative and convective heat transfer within the combustion zone, moisture also will increase the burning time by reducing radiation to the particles (King, 1973). It is noted that the effects of M on particle ignition time and particle burning time are sometimes difficult to separate because a fraction of M is lost in preheating and the remainder is lost during particle consumption by flaming combustion. Research has not yet clarified how moisture change takes place while a fuel layer burns, but the relative amounts of water lost during preheating and flaming combustion seemingly would depend on particle size, shape, and arrangement and on the initial value of M (i.e., on the amounts of liquid and/or adsorbed water present).

C. Fuel Characteristics Affecting Moisture Content

If the effects of weather are disregarded, the most significant factors affecting the amount of water held and transported in woody and vegetative particles are chemical composition, internal structure, and physical properties. In the case of a fuel bed, several layer characteristics may be significant also. The amount of moisture held in the cell walls of fuel particles is related to composition and crystalline structure of the walls, whereas the liquid water held in the cell cavities is determined by the larger scale capillary structure.

1. Chemical Composition

The chemical constitution of wood is similar to that of foliage. Stamm and Harris (1953) give the cell wall composition of wood on a percentage of dry weight basis as cellulose (40–55%), hemicellulose (15–25%), lignin (15–30%), and extraneous and extractive matter (2–15%). Extractives include various organic compounds such as resins, sugars, and fatty acids that may be soluble in either alcohol, water, or organic solvents (e.g., xylene or ether). The only mineral constituent they cite is ash with a content between 0.1 and 4%. Thus, the holocellulose content (cellulose plus hemicellulose) ranges from about 55 to 80%. When ranked according to their hygroscopicity (or affinity for water), these components are ordered as hemicellulose, cellulose, lignin, and extractives. On the other hand, foliage contains the same components but in different amounts. According to Susott (1980), the range in composition of old and new needles of three western conifers is holocellulose (35–44%), lignin (18–19%), and extractives (37–47%). The higher percentage of extractives in needles than in wood tends to reduce water takeup and rates of moisture exchange (Anderson,

1990a, 1990b). Yet, the experimental data of Anderson (1990b) tend to confirm the results of earlier investigators (Dunlap, 1932; Blackmarr, 1971), showing that forest fuels are slightly more hygroscopic than wood under identical conditions of air temperature and relative humidity. This could be the case if the tendency toward smaller moisture contents due to smaller hemicellulose content of the fuels is more than offset by the fact that the hygroscopicity of hemicellulose exceeds that of wood cellulose by 50% (Browning, 1963); alternatively, the extractives in some conifer needles and deciduous leaves may be more hygroscopic than wood holocellulose. As litter fuel weathers over time, water-soluble extractives are leached from the surface and interior of the particles, and the holocellulose content is reduced due to consumption by microorganisms. This loss of dry mass can be approximated as an exponential decrease with time (Olson, 1963).

2. Internal Structure

The instantaneous level of moisture content in forest fuels is strongly influenced by the internal structure of the material and by whether the fuel is alive or dead. The factors controlling water movement in living plants are osmotic forces due to intercellular differences in plant water concentration and capillary tension forces created by transpirational demand at the external surfaces of the leaves (the term "leaves" includes conifer needles also). This demand for water must be satisfied primarily through absorption by the roots. In dead fuel particles, the most significant factors are two transport properties: (1) the permeability of the fuel to liquid water (bulk flow in cell cavities by capillarity), and (2) the moisture diffusivity (molecular flow in cell walls by bound water diffusion or in air spaces by diffusion of water vapor). An additional factor in litter and duff layers is liquid water drainage due to gravitational forces.

a. Live Fuels

The cells in living fuels contain protoplasm, cell wall material, and one or more vacuoles. The living protoplasm is largely made up of water, protein, various dissolved organic compounds and salts (cytoplasm), and a nucleus that controls inheritance and the metabolic activity of the cell through the genes it contains. The vacuole is located within the cytoplasm and is filled with cell sap (about 98% water plus various dissolved compounds). The watery solution surrounded by the nonliving primary cell wall is called the *protoplast*. The wall itself is mainly composed of cellulose, hemicellulose, and pectin; the water it contains is referred to as the *apoplast*. As the cell matures, the vacuole enlarges and eventually occupies most of the cell (Figure 1). Water movement in the cell is accomplished primarily by osmosis, for which the thin outer layer of cyto-

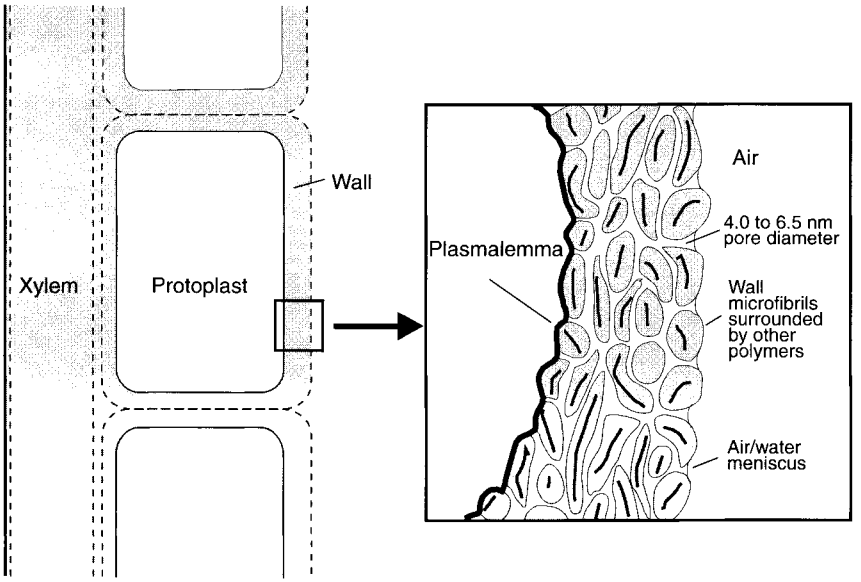

FIGURE 1 Mature cell wall showing the xylem through which water flows and the protoplast in the vacuole. The enlarged inset shows the apoplast, including air-water interfaces between the polymer microfibrils. The plasmalemma is pressed against the wall from the inside and pulled in the same direction by tension from the outside. This is the source of plant turgor. Adapted from Kramer and Boyer (1995).

plasm in contact with the cell wall interior, the *plasmalemma,* functions as the semipermeable membrane. In general, any given cell is surrounded by other cells or by a solution containing various solutes. Hence cell A with higher solute concentration than cell B will have a lower water concentration than cell B so that water will move from B to A by osmosis. Cell A will become turgid and cause the cytoplasm to press against the cell wall. This is the origin of "turgor pressure." In the opposite sense, when water leaves cell B, the cytoplasm shrinks from the cell wall, and if carried to the extreme, cell B dies. In addition to osmosis, liquid imbibition (or absorption) within the cell wall occurs in live or dead cells. The influence of the fine structure of the wall on this process is discussed in the next section.

In living fuels, liquid soil water absorbed by the roots moves by capillary flow through the water-conducting xylem of the stem, into the leaves, and then into the atmosphere through the leaves as water vapor. The processes of liquid absorption and vertical ascent are highly significant because they can limit the rate of water supply to the leaves by reducing plant turgor and causing stomatal closure. Figure 2A shows the structure of a deciduous leaf and pathways for

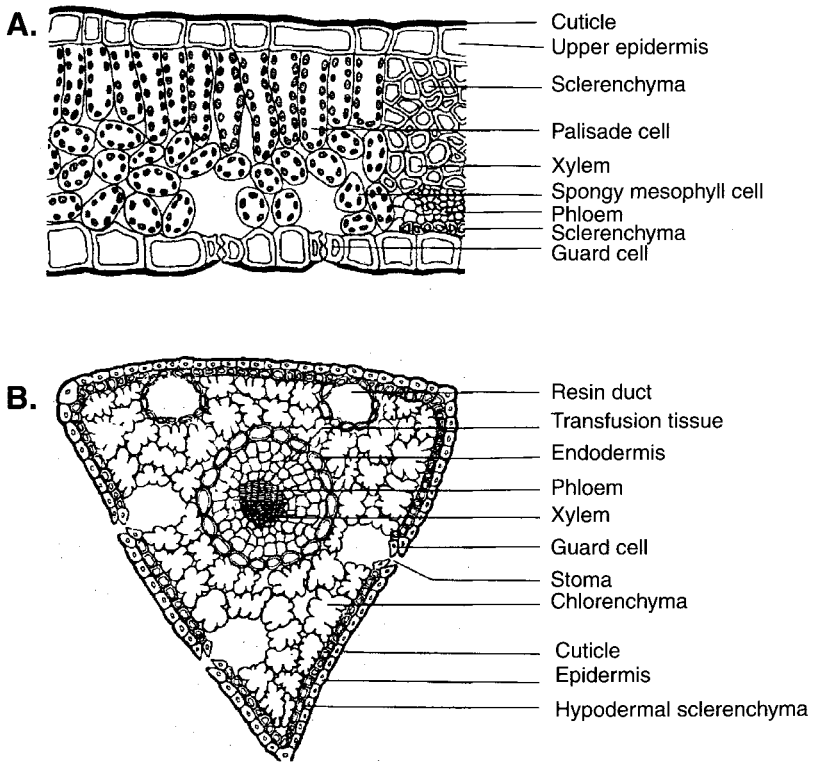

FIGURE 2 Structure of leaves from a deciduous tree and a conifer. Water vapor loss is primarily through the internal air spaces and guard cells, with a small amount of vapor diffusing directly through the epidermis and cuticle: (A) species not identified, (B) eastern white pine. From Kramer and Kozlowski (1979) and Kozlowski and Pallardy (1997), respectively.

liquid transfer. Food, water, and nutrients are supplied to and removed from the leaf through veins (not shown) that penetrate the mesophyll (palisade and spongy parenchyma) cells. These cells, in which photosynthesis occurs, are surrounded by a network of small intercellular spaces; other spaces just behind the lower epidermis are relatively large. These air spaces create a large amount of internal surface from which evaporation can occur. The vapor then diffuses toward and through the guard cells surrounding the stoma and into the atmosphere. This process is referred to as *stomatal transpiration.* A small amount of vapor also exits the leaf through the epidermal layers but is reduced by surface cuticle—*cuticular transpiration.* The stomates are found on both sides of the leaves but generally are more numerous on the underside. Conifers, with the exception of pines, also produce needles in which the mesophyll consists of

palisade and spongy parenchyma cells. The pine needle cross section in Figure 2B shows sclerenchyma cells which provide mechanical support and chlorenchyma cells that contain chloroplasts. The transfusion tissue is involved in solute transport.

If the supply of water is not a limiting factor, the two major sources of resistance to evaporation are associated with the leaf and the atmosphere. The former resistance primarily is due to covering of the leaf surfaces by a relatively waterproof layer of cutin and wax (cuticle) and to stomatal resistance related to size of the aperture. In pine species, wax also is present in stomatal chambers. Aperture size of the stomates strongly depends on plant stresses and environmental factors such as sunlight, air temperature, and relative humidity. Atmospheric resistance is due to the leaf boundary layer, a thin region adjacent to the surfaces in which the factors affecting transport of vapor into the atmosphere are changing from leaf values to atmospheric values. This resistance, determined by particle size and shape and by wind speed, decreases as air flow over the particle increases. More information on water transport as related to the internal structure of living fuels may be found in texts such as Slatyer (1967), Kramer and Boyer (1995), and Kozlowski and Pallardy (1997).

b. Dead Fuels

The amount of moisture held in the cell walls of live or dead fuels (as discussed earlier in connection with cell wall imbibition) is related to the fine-scale structure of the walls. Approximately 50 individual cellulose chains are held together in parallel chance groupings by hydrogen bonds and various other types of secondary bonding to form a crystalline region, or crystallite. These elements are thought to be about 0.06 μm long—much shorter than a cellulose chain—due to the frequent occurrence of amorphous regions between the crystallites. The amorphous regions are regions in which the chains are highly disordered. Thus individual chains pass through several crystalline and amorphous regions but are linked at only a few points in the amorphous regions so that most of the active hydroxyl groups are available to take on water molecules. This water then forces the chains farther apart and swells the material. Because water is adsorbed throughout the amorphous regions but only on the surfaces of the crystallites, the water-holding ability of the cellulose varies directly with the proportion of the cellulose that is amorphous. The crystallites, with their associated amorphous regions, become further aggregated into fibrils that are embedded within the lignin-hemicellulose matrix materials to make up the various layers of the cell wall. In these fibrous materials, a secondary wall (the S_1, S_2, and S_3 layers) composed mainly of cellulose is found inside the primary wall and provides structural integrity (Figure 3A). In wood, the S_2 layer makes up 60–80% of the cell wall, thus controlling shrinkage, swelling, and other physi-

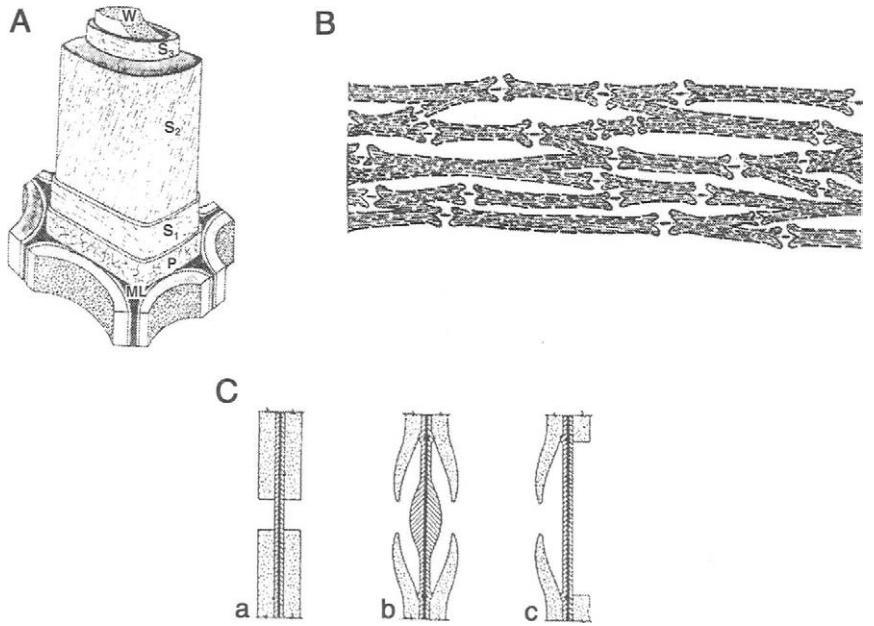

FIGURE 3 Structural features of a softwood. (A) View of a mature tracheid in which ML is the middle lamella that cements tracheids together, P is the primary wall, S_1, S_2, and S_3 are secondary walls, and W is the "warty" layer of unknown composition. From Coté (1967). (B) Pathways for continuous liquid or vapor flow through the large white cell cavities and bordered pits and for intermittent bound water/water vapor flow through cavities and the darker cell walls (the middle lamella between tracheids is not clear). From Stamm (1946). (C) Three kinds of pit pairs—a, simple pit with the dark middle lamella, cross-hatched primary wall, and dotted secondary wall; b, bordered pit with the torus midway in the pit membrane; c, half-bordered pit with no torus. Reproduced with permission of The McGraw-Hill Companies from Brown, H. P., Panshin, A. J., and Forsaith, C. C. (1949). "Textbook of Wood Technology, Vol. 1," 1st ed. McGraw-Hill, New York.

cal properties (Siau, 1995). References on details of the fine-scale structure of wood and cellulose are Browning (1963) and Panshin and de Zeeuw (1980).

The fractional moisture content M of dead fuel particles can reach maximum values between 2.5 and 3, depending on the wood or foliage particle specific gravity (Stamm, 1964). Both types of fuel exhibit sudden changes in moisture transport mechanisms and in electrical, mechanical, and thermal properties when M is in the range 0.21 to 0.35. These changes are associated with a value of M called the *fiber saturation point* that may be estimated for each fuel; the variability in its value can be due to differences in fuel temperature, mechanical stress, specific gravity, or chemical composition. The fiber saturation point, M_{fsp}, has been defined in various ways. It is most often defined as that M value obtained when isothermal equilibrium data for M are plotted as a function of

increasing fractional relative humidity, H, and then extrapolated from $H = 0.95$ to $H = 1$ (Stamm, 1964). This procedure estimates the M value at which the fuel cell walls are saturated but no condensed water exists in the capillary structure. The method is an idealization, however, because there is no abrupt transition from a "saturated cell wall" region to a "liquid water" region; instead, the transition occurs over a range in H from about 0.9 to 0.995. Above the latter value, the fuel becomes increasingly saturated. The figure generally used for M_{fsp} by fire researchers is 0.30, independent of fuel type or state.

Gain or loss of moisture by dead fuel particles above M_{fsp} occurs by movement of liquid water through the fuel capillary structure in response to surface tension forces. The specific permeability (m^2) of a porous material is a measure of the ease with which fluids can move in bulk through the material in response to a pressure gradient in the fluid. In woody and vegetative particles, permeability to water depends on the internal structure of the material and extent of its swelling. Because forest fuels usually exchange moisture with the atmosphere at temperatures below 60°C, vapor pressure differences are not extremely large, and moisture transfer by gas flow often is considered negligible in comparison with that due to liquid flow. In softwoods, passage of liquid water is through fiber cavities in series with tiny holes in the pit membrane called pit membrane pores; on the other hand, continuous liquid movement through the permanent cell wall capillaries contributes little to the overall flow (Stamm, 1964). Figure 3B is a sketch of the gross capillary structure of a softwood and paths for liquid transport through fiber cavities and pit membrane pores. Darkened areas represent a network of lignocelluosic strands (or fibrils) intertwined to form the cell wall, whereas the white areas represent fiber (or tracheid) cavities and pit chambers within the bordered pits. Figure 3C shows three types of pit pairs found in softwoods and hardwoods. Bordered and half-bordered pits are common in softwoods, whereas simple pits occur in hardwoods. The enlarged region in the center of the pit membrane is called the torus; the pit becomes aspirated when the torus is sealed against a border by surface tension forces created in drying (Hart and Thomas, 1967). The pits also can become impervious to water because of encrustation by extractives.

The internal structure and liquid permeability of hardwoods is more complex and more variable than that of softwoods. The primary conducting elements, or vessels, are interspersed among tracheids and other fibers and interconnected by simple pits. Resistance to liquid flow is offered by the pits and by internal growths, or tyloses, lodged in the vessels of most species. In the pits, resistance is due to encrustation rather than aspiration because pits in hardwoods have no torus in the pit membrane. Furthermore, the openings in the pit membrane are about 10 times smaller in hardwoods than in softwoods, but not so small as to prevent water flow. One of the most permeable woods is red oak (no tyloses) with a longitudinal permeability of about 2×10^{-10} m^2. The sapwood and heartwood of many softwoods and hardwoods exhibit longitudinal

permeabilities ranging from 10^{-12} to 10^{-15} m^2. Comstock (1970) measured longitudinal/tangential permeability ratios in softwoods ranging from about 500 to 8×10^4. Siau (1995) refers to an unpublished study of eight hardwoods by Comstock reporting longitudinal/tangential permeability ratios between 3×10^4 and 4×10^8. Additional information concerning flow pathways and the relation of internal structure to fluid flow in wood may be found in Stamm (1964) and Siau (1995).

The flow of liquid water in layers of deciduous or coniferous litter and duff is determined by the amount of moisture retained on and within the particles and in the interstices between particles. In a series of laboratory experiments, Stocks (1970) applied simulated rainfall amounts ranging from 12.7 to 50.8 mm to air-dry ponderosa pine duff layers 7.6 cm thick at a rate of about 25.4 mm h^{-1}. The results showed that the percentage of the applied rainfall retained by the duff decreased from 20 to 11% as rainfall amount increased. When the laboratory experiment was repeated using moist duff, water retention was halved and the percentages decreased from 10 to 5% as rainfall increased. Stocks (1970) also reported field and laboratory experiments suggesting that the moisture content of the duff in a thin sublayer adjacent to underlying mineral soil is smaller than in the sublayers just above it (Figure 4). These results are consistent with

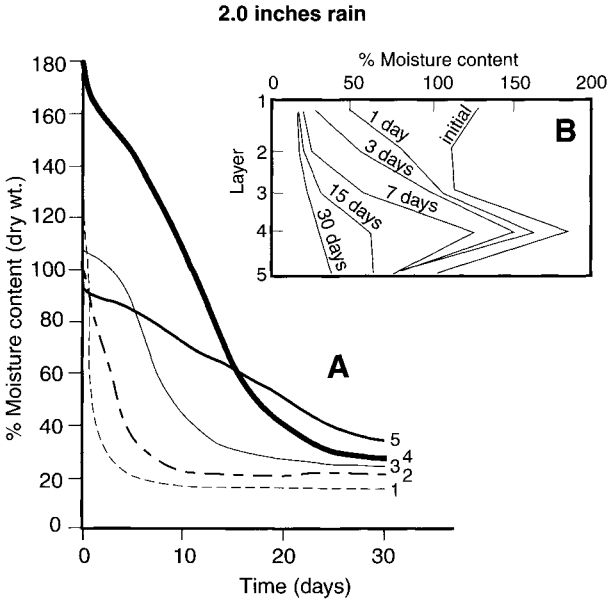

FIGURE 4 Laboratory drying rates for five separate sublayers within a 7.6-cm duff layer (primarily ponderosa pine) after 50.8 mm (2 inches) of simulated rain. "Layer 1" is at the top of the duff layer. (A) Moisture content versus time after rain. (B) The vertical distribution of moisture content for specific times after rain. Adapted from Stocks (1970).

the idea that the amount of rainfall retained by the layer depends on a balance among capillary forces across the duff-soil interface, capillary forces among the fuel particles, gravitational forces acting over the vertical depth of the layer, and attractive forces drawing water into the particles. Structural details of the layer affect this balance by determining the specific permeability of the duff. Fosberg (1977) measured the permeability of several western conifer duff layers to air and reported values ranging from about 10^{-8} to 5×10^{-11} m^2. These values are orders of magnitude larger than those for wood, reflecting the much larger sizes of the conducting pores.

Moisture diffusivity ($m^2\ s^{-1}$) is the property that governs exchange of moisture in dead fuel particles below M_{fsp}. Water movement is due to combined diffusion involving a gradient in bound water concentration across the cell walls and a gradient in partial vapor pressure through the fiber cavities and pit membrane pores. Stamm (1964) states that bound water diffusion differences between softwoods and hardwoods are small, so diffusion of vapor through the continuous void structure is the major source of variability among species. Stamm (1964) and Choong (1965) suggest, however, that in softwoods the percentage of the transverse moisture diffusion attributable to vapor diffusion is 22% or less at temperatures below 50°C. Thus structural differences between softwoods and hardwoods normally cause only small differences in diffusional flow. Though the circumstances under which diffusion operates in dead foliage particles are not well known, equilibrium and dynamic moisture relationships in these fuels are well represented in form, if not in magnitude, by research results for wood over a large range in M. This is verified to some extent in data reported by Van Wagner (1979) on drying of jack pine litter that are similar to those from studies on wood and paper (Nelson, 1969). Other data demonstrate, however, that diffusivities differ for particles of wood and foliage. Values of the integral moisture diffusivity (the average value for the particle or layer), D_{av}, observed by Linton (1962) for *Eucalyptus obliqua* wood ranged from 1.4 to 42×10^{-11} $m^2\ s^{-1}$ for twigs 6 mm in diameter and from 3.5 to 45×10^{-12} $m^2\ s^{-1}$ for twigs 3 mm in diameter. Linton also found that individual leaves from *Eucalyptus obliqua* and *Eucalyptus radiata* exhibited D_{av} values ranging from 0.24 to 11×10^{-12} $m^2\ s^{-1}$. Anderson (1990a) reported a comprehensive study in which grasses, hardwood leaves, conifer needles, and square softwood sticks initially in equilibrium at 26.7°C and H of 0.9 were subjected to a rapid drop in H to 0.2 at which they equilibrated and then were exposed to another step change in H back to 0.9. Weathered foliage fuels were studied also. Results showed that D_{av} of the wood ranged from about 0.1 to 2×10^{-10} $m^2\ s^{-1}$, in good agreement with measurements of transverse diffusion in softwoods and hardwoods for which D_{av} ranged from 0.07 to 1.7×10^{-10} $m^2\ s^{-1}$ (Stamm, 1960; Simpson, 1993a). On the other hand, Anderson's foliage diffusivities (for recently cast fuel) ranged from about 10^{-14} to 10^{-12} $m^2\ s^{-1}$. These values are in

approximate agreement with the observations of Linton (1962), but even Anderson's values for weathered fuels (10^{-13} to 10^{-12} m^2 s^{-1}) are smaller than those for wood by two orders of magnitude.

3. Physical Properties

The differences in moisture diffusivities of dead wood and foliage just described are due, at least in part, to differences in mass density, particle size and shape, and extractive content. Moreover, the effects of weathering on moisture relationships operate primarily through these variables. The density of wood depends on its specific gravity and moisture content, ranging from about 300 to 800 kg m^{-3} (Simpson, 1993b); values for foliage fuels fall well within this range (Anderson, 1990a). The effect of density on diffusion has not been identified in experimental studies. Though he acknowledged the lack of conclusive data, Hart (1964) argued that two samples of wood drying in response to identical gradients in M will exhibit diffusivities inversely proportional to their densities. Particle density also is affected by water-soluble extractives that, because of their bulking action, leave the fiber cell wall in an expanded state when drying from the green condition takes place. For foliage, this effect may be overshadowed by the flow reduction due to wax on particle surfaces. Van Wagner (1969a) presents data showing that *response time* τ (s) (the time required for accomplishment of $1 - 1/e$, or 63.2%, of the total moisture content change due to a step change from a constant initial value to a constant final value) decreased by factors averaging about 5.5 and 2.5 for red pine needles and aspen leaves that had been pretreated with xylene to remove the waxes and resins. This result implies that fuel particles with surface wax removed by weathering will gain or lose moisture about three to six times faster than unweathered particles whose surface wax is intact.

The effects of particle size are best obtained from the theory of diffusion in solids (Crank, 1975). The diffusion theory, discussed briefly in Section III.D.2, indicates that the theoretical effect of minimum particle dimension d (m) on D_{av} is zero because the local diffusivity, D, is treated as a constant and therefore equals D_{av}. Dimension d usually is the radius of a cylinder (or sphere) or the half-thickness of a slab. It is well known, however, that D_{av} for wood is not constant, but a function of moisture fraction M and fuel temperature T_f.

The measurement of D_{av} is further confounded by the possible occurrence of two nondiffusional mechanisms that can be mistakenly interpreted as diffusion. The first of these involves the slowing of *sorption* [this term is used when reference is made to the combined processes of adsorption and desorption (see Section III.D.1) or when no distinction between the two processes is necessary] due to molecular rearrangements associated with relaxation of shrinkage or swelling stresses. These rearrangements are more pronounced during adsorption in

thin particles ($<$ 3 mm thick) when fractional humidity H exceeds 0.5; they make new adsorption sites available at a slower rate than the initial diffusion rate (Christensen, 1965). The second mechanism is moisture transfer at the solid surface. The theoretical influence of this process is expressed in terms of the dimensionless mass transfer Biot number, Bi—the ratio of resistance to moisture transfer at the surface to that within the particle. This number is discussed further in Section III.D.2. Byram (1963, unpublished) expressed the results from classical theory in terms of response time and found τ proportional to d^2 when Bi approaches infinity. For smaller Bi, approaching zero, τ was predicted as proportional to d. Nelson (1969) tested Byram's predictions with laboratory drying experiments on cellulosic materials exposed to fixed step changes in H at constant temperature. Two values of τ were observed for most runs. The τ versus d^2 relationship was approximated for sawdust layers (τ depended on $d^{1.8}$ rather than d^2), square wooden sticks, and thin slabs of paper (during the later stage of drying) for initial values of M well above M_{fsp}. The approximate d^2 dependence observed in all fuels studied suggests that diffusivity D_{av} was nearly independent of d in these tests. Results for the paper slabs are presented in Figure 5. The data show that the predicted τ versus d result was observed in approximate form (τ depended on $d^{1.27}$ rather than d) during the early stage of drying when the resistance to transfer at the surface must have exceeded that within the slabs. For the two thinnest slabs, the tendency for τ to become independent of d indicates that the drying rate depended entirely on the external conditions. In other work, the effect of thickness on moisture change in *Eucalyptus regnans* sapwood specimens was studied by King and Linton (1963) who found that τ increased with increasing d, but not according to d^2 as would be expected from theory. Taken together, the data suggest that the predicted effects of d on τ will be approximately correct for forest fuels and that D_{av} is nearly independent of d in the diffusion-controlled range when external conditions are constant.

Particle shape theoretically affects moisture exchange by means of differences in constants derived in analytical solutions of the equations describing diffusion in the various particles. In practice, these effects due to shape operate partly through Biot number Bi and partly through the particle *surface-to-volume ratio* σ (m^{-1}) that influences the exchange of heat and mass between the particle and the surrounding fluid. Larger values of the ratio result in larger exchange rates because of increasing surface area per unit of particle volume. This ratio is one of the factors defining the openness of fuel layers which, in turn, may determine the rate-controlling dimension during moisture exchange. A second controlling factor, the dimensionless fuel bed *packing ratio*, β, represents the volume of fuel particles within unit volume of fuel bed. An interesting question not yet answered by research is the following: if a fuel layer of constant packing ratio β, vertical depth δ (m), and uniformly distributed cylindrical particles of radius d (or constant σ) is exposed to a step change in H at constant T,

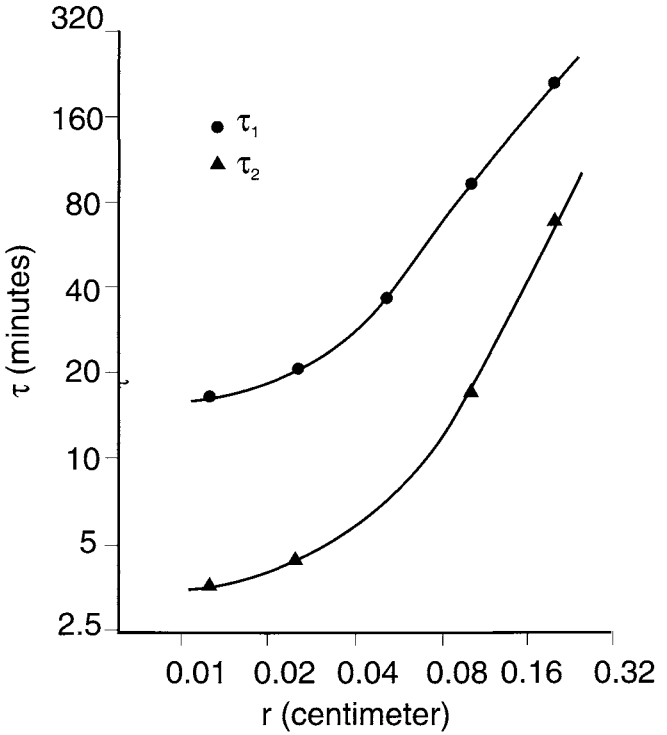

FIGURE 5 Logarithmic plot of response time versus total thickness of paper slabs drying at 27.2°C and 36% relative humidity, where τ_1 refers to early drying when surface effects were present but not dominant and τ_2 to the later stages when internal diffusion was controlling the process. For small values of slab thickness, response time tends to become independent of thickness due to surface control. From Nelson (1969).

is its rate of moisture exchange controlled by δ or d? Though the answer to this question partly depends on the imposed boundary conditions, in general one would expect that moisture gain or loss in tightly packed beds is controlled by δ, and that as β decreases and the beds become more open, the rates of moisture exchange would approach the rate for a single particle. The limited data of Anderson *et al.* (1978) for beds of ponderosa pine needles suggest this is so. In later work, Anderson (1990a) compared the diffusivities of layers with different degrees of packing with those of widely spaced needles drying in similar environmental conditions and found that D_{av} decreased as the fuel beds became deeper or more dense. Using the method of nonlinear least squares, Anderson also developed equations for predicting the effects of fuel particle and fuel bed variables. He produced four groups of equations—each group distinguished by

the hardness of wax on the fuel surfaces or by the amount of surface cuticle. Within each group, equations were developed for recently cast and weathered fuels undergoing adsorption and desorption. All equations showed that response times were proportional to the quantity $\sigma^a\beta^b\delta^c$, where exponents a, b, and c differed among fuel species and sorption conditions. Anderson stated that increasing β and δ when σ is constant decreases D_{av} and increases τ, and that additional study is needed.

III. FUEL MOISTURE RELATIONSHIPS

The moisture content of living fuels involves free water and water vapor in plant void spaces and in the cell walls and surrounding tissues. For example, an equilibrium relationship between water content and water potential describes water retention in plant tissue, bulk capillary flow takes place in the stems of woody plants, and water exits the interior of leaves by vapor diffusion (Kramer and Boyer, 1995). Similar phenomena take place in dead fuels. Approaches for describing moisture held at equilibrium in hygroscopic porous solids range from empirical and semiempirical models to rigorous theories based on the physical chemistry of solutions or statistical thermodynamics. Water movement in porous bodies, including dead forest fuels, can be described mathematically in two ways. In the first, water transport is assumed to obey the conservation equations of engineering mechanics (Spolek and Plumb, 1980). The second approach involves the procedures of nonequilibrium thermodynamics (Katchalsky and Curran, 1965). The underlying foundation of this method rests in the conservation equations of mass and energy and in the thermodynamic laws but involves additional assumptions about the conservation of momentum and deviations from equilibrium. The primary driving force for mass flow is the spatial gradient of the partial molal Gibbs free energy; this idea has been accepted by soil and plant water researchers for many years and now is drawing the attention of wood-drying researchers (Cloutier and Fortin, 1991, 1993; Siau, 1995; Zhang and Peralta, 1999). The rapidly developing thermodynamic methods, which have been little used in forest fuel moisture research, are not discussed further because of space limitations.

A. Water Potential

Researchers studying water relationships in soils and plants as separate thermodynamic systems have long recognized that water tends to move in these materials from regions of high Gibbs free energy to regions of lower free energy. This is consistent with the thermodynamic concept of equilibrium which tells

us that two bodies (or two regions within a single body) are in equilibrium only when the Gibbs free energy difference between them is zero. Water moves across the soil–atmosphere, soil–plant, and plant–atmosphere interfaces in response to free energy gradients, so viewing the three separate domains as one unified thermodynamic system is a logical research approach. This single-system concept has been labeled SPAC to refer to the "soil–plant–atmosphere continuum" and has been accepted by many workers in the two subject matter areas.

The energy status of water in living or dead plants, soils, or the atmosphere measures the potential energy of the water in its current state when temperature, pressure, and chemical composition are the only variables. This energy is the partial molal Gibbs free energy, or chemical potential, μ (J mol^{-1}). The standard reference state in both soil and plant water research, denoted by μ_0, is taken as pure liquid water at atmospheric pressure and at the temperature of water in the material. The reference location is an arbitrarily chosen elevation. Because water is essentially incompressible (except at very small moisture fractions), its density (kg m^{-3}) and molecular weight (kg mol^{-1}) can be used to express μ in units of pressure, J m^{-3}. Thus water potential ψ is defined as

$$\psi = \rho_w(\mu - \mu_0)/M_w = (\mu - \mu_0)/V_w \tag{3}$$

where ρ_w, M_w, and V_w are, respectively, the density, molecular weight, and molar volume of liquid water and μ and μ_0 are chemical potentials of water in the plant and in the reference state. For plant water in the reference state, $\psi = 0$. The water potential ψ (J m^{-3}), applicable in both soils and plants, is written as

$$\psi = \psi_p + \psi_m + \psi_s + \psi_g \tag{4}$$

where ψ_p is the pressure potential owing to plant turgor (hydrostatic forces in excess of those due to atmospheric pressure acting on cell walls and internal membranes), ψ_m is the matric potential caused by capillary or binding forces at internal surfaces of cell walls, ψ_s is the osmotic potential due to a reduction in water vapor pressure by solutes and surface attraction, and ψ_g is the gravitational potential which originates from the difference in gravitational force acting on water at a given location and at the reference location. In general, ψ_g is taken to be negligible in the water of living plants, and ψ_p is considered to be zero in soil water. Cowan (1965) and Philip (1966) were among the early workers who attempted to describe water flow in living plants with physical coefficients like diffusivity and conductivity, but within the continuum framework. Lemon *et al.* (1971) and Riha and Campbell (1985) are other modelers who have used a similar approach. References summarizing the SPAC concept and research on water transport in plants are Kramer and Boyer (1995) and Kozlowski and Pallardy (1997).

B. Conservation Equations

Though the conservation laws are equally applicable to live fuels, they are discussed here in the context of dead fuels because their application to water transport problems in these fuels is relatively simple. The solid fuel and its associated moisture comprise four separate phases: the dry solid, free liquid water, bound liquid water, and a gas phase consisting of a mixture of dry air and water vapor. Equations expressing the conservation of mass, momentum, and energy may be written for each phase. The intricate chemical and structural features of fuel particles or layers require the moisture exchange modeler to consider carefully the elementary volume selected as the basis for writing equations governing the process. Though a set of differential equations can be written to describe changes within each phase in the system, it is not possible to know which set to assign at each point in the medium. One approach to this problem is to define an elementary volume within the particle just large enough to contain all phases and satisfy the definitions of all system variables. Then a set of volume-averaged equations may be written that should be valid at all locations and the fuel-water system may be treated as a continuous medium (Spolek and Plumb, 1980). This procedure is known as *local volume averaging* and has been used by several researchers to describe heat and mass transfer in wood. Perre *et al.* (1990) pointed out that moisture transport in wood at temperatures between 60 and 120°C is best considered a low- to moderate-temperature process taking place with variable total pressure. On the other hand, an assumption of constant total pressure may be reasonable for open duff layers or for moderately thin fuel particles because within-particle temperatures, even in intense sunshine, seldom exceed 60°C, and the internal pressure does not differ greatly from atmospheric. Perre *et al.* also assume thermal equilibrium among all phases—an assumption that is commonly used because of the mathematical simplification it provides.

In the present discussion, we consider the unaveraged equations (equations for each phase) that would describe heat, mass, and momentum transfer in an elementary volume of fuel particle. Suppose that shrinking and swelling of the particle are ignored and gravitational body forces, kinetic energy changes, and the rate of doing work on the water are negligible. Then the equation that balances the transport of phase i in direction x (m) in a plane body (a slab, for example) may be written as

$$\partial(\rho_i\phi_i)/\partial t = -\partial(\rho_i\phi_i v_i)/\partial x - w_i = -\partial(J_i)/\partial x - w_i \qquad (5)$$

where ρ_i (kg m^{-3}), ϕ_i, v_i (m s^{-1}), and w_i (kg m^{-3} s^{-1}) are the density, volume fraction, velocity, and evaporation rate of phase i—all on a unit volume of particle basis—referred to a coordinate system on the stationary particle. The mass fluxes J_i (kg m^{-2} s^{-1}) take forms that depend on the transport mechanism for phase i. Subscript i ($i = s, w, b, g$) denotes the solid, free liquid, bound liquid,

or gas phase, respectively. The dry air component of the gas phase, indicated by subscript a, can be described with its own mass conservation equation given by

$$\partial(\rho_a \phi_a)/\partial t = -\partial(\rho_a \phi_a v_a)/\partial x = -\partial(J_a)/\partial x \tag{6}$$

where $w_a = 0$. In addition, the diffusion flux of air can be written as

$$J_a = -\rho_a \varepsilon D_v \partial[\ln(P_T - P_v)]/\partial x = -\rho_a \varepsilon D_v \partial[\ln(P_a)]/\partial x \tag{7}$$

where εD_v ($m^2\ s^{-1}$) is the diffusivity of water vapor in air (or air in water vapor) corrected for presence of the solid (ε is the void fraction) and total gas pressure P_T depends on the partial pressures of air and vapor, P_a and P_v, according to

$$P_T = P_a + P_v \tag{8}$$

Equality of temperatures T_a and T_v of the two gases and applicability of the ideal gas law are assumed.

For moisture change in forest fuels, it is usually not necessary to include equations for momentum conservation explicitly because flow rates are slow and fuel temperatures rarely exceed 60°C. Though the transport relationships describing J_i (Fick's law and Darcy's law) may be derived from approximate expressions of momentum conservation, their origin is empirical because of their discovery during 19th century experiments. The equations for J_i, where $i = w$, b, v (v denotes the water vapor component of the gas), may be written as

$$J_w = -(K_w/\eta_w)\partial(P_w)/\partial x = -(K_w/\eta_w)\partial(P_T - P_c)/\partial x \tag{9}$$

$$J_b = -\rho_s m D_b \partial[\ln(P_b)]/\partial x \tag{10}$$

$$J_v = -(K_g/\eta_g)\partial(P_T)/\partial x - \rho_v \varepsilon D_v \partial[\ln(P_v)]/\partial x \tag{11}$$

where K_w (m^2), η_w ($m^2\ s^{-1}$), and P_w ($J\ m^{-3}$ or $kg\ m^{-1}\ s^{-2}$) in Eq. (9) are the specific permeability of the medium to liquid water and kinematic viscosity and pressure of the liquid phase. This equation is Darcy's law describing movement of liquid water in an unsaturated two-phase system by capillary forces. Capillary pressure P_c ($J\ m^{-3}$) is the pressure difference at a gas-liquid interface given by

$$P_c = (P_g - P_w) = (P_T - P_w) = 2\gamma/r \tag{12}$$

where γ is the surface tension of the liquid and r is the mean radius of the interface (Siau, 1995). Equation (10) originates in the equation of motion for the adsorbed phase (Babbitt, 1950; Nelson, 1986b) and describes bound water diffusion in the cell walls. Quantities ρ_s ($kg\ m^{-3}$), D_b ($m^2\ s^{-1}$), m, and P_b ($J\ m^{-2}$) denote the density of the dry particle, bound water diffusivity, local moisture content fraction, and spreading pressure of water in the cell wall. The two-dimensional spreading pressure of a film adsorbed on the internal surface of a solid is analogous to the pressure of a three-dimensional gas in that adsorbed water molecules jump from one sorption site on the surface to another because of differences in film surface tension. Terms on the right side of Eq. (11) account

for the capillary flow and diffusion of water vapor in the medium. Quantities K_g (m^2), η_g ($m^2\ s^{-1}$), ρ_v ($kg\ m^{-3}$), and εD_v ($m^2\ s^{-1}$) refer to the specific permeability of the medium to gas flow, kinematic viscosity of the gas, density of the vapor, and corrected vapor diffusivity. Equations (9)–(11) may be substituted into Eq. (5) to obtain the within-phase equations of moisture transport. When $i = w$ in Eq. (5), $w_i = w_w$; when $i = b$, $w_i = w_b$; when $i = g$, $w_i = w_g = w_v = -(w_w + w_b)$ and the interphase sink/source terms sum to zero.

The conservation of energy within phase i may be written as

$$\rho_i \phi_i c_i \partial T_i/\partial t + c_i J_i \partial T_i/\partial x + w_i \lambda_i = -\partial q_i/\partial x = \partial(k_i \partial T_i/\partial x)/\partial x \qquad (13)$$

where c_i ($J\ kg^{-1}\ K^{-1}$) and T_i (K) are the constant-pressure specific heat and temperature of phase i, λ_i ($J\ kg^{-1}$) is the heat of evaporation/condensation of phase i, k_i ($J\ m^{-1}\ s^{-1}\ K^{-1}$) is the thermal conductivity, and q_i ($J\ m^{-2}\ s^{-1}$) is the heat flux that accounts for all mechanisms of heat transfer to the phase. In Eq. (13), it is assumed that conduction is the only means of heat transfer, and use is made of another empirical relationship—the Fourier law of heat conduction. Equation (13) must be summed over all phases (assuming local thermal equilibrium) because all are capable of transferring heat. It is noted that $J_s = w_s = w_a = \lambda_s = \lambda_a = 0$; in addition, $\lambda_b = (\lambda_w + \lambda_d)$, where λ_d ($J\ kg^{-1}$) is the differential heat of sorption. A discussion of general wood–water thermodynamic relationships, including the differential heat of sorption, is given by Skaar (1988).

Consistent with their application and the desired level of complexity, Eqs. (5)–(13), or a subset of them, may be solved analytically or numerically in conjunction with fixed or variable boundary conditions involving one or more of the following variables: moisture content, temperature, relative humidity, wind speed, solar radiation, and net longwave radiation from various sources. Use of these equations requires still more information that includes expressions for void fraction, transport properties, thermal properties, and thermodynamic relationships. For multiple phases, relative amounts of space occupied by free water and water vapor are needed. Examples of the incorporation of this kind of information into models describing multiphase transport through volume averaging are the studies of Spolek and Plumb (1980), Perre *et al.* (1990), and Fernandez and Howell (1997).

C. Live Fuel Moisture

The understanding of water retention and movement in plants and in the soil supporting their growth is basic to development of models for predicting the moisture content of live surface and crown fuels. These models would help forest fire management and control personnel quantify the behavior of crown fires and anticipate the transition from surface fire to crown fire. Testing of a crown

fire spread model that uses fuel moisture content as an externally supplied input parameter is underway (Alexander *et al.*, 1998).

1. Moisture Characteristic Curves

The equilibrium relationship between plant tissue water content and water potential at constant temperature is often referred to as the moisture characteristic curve by plant water researchers, and similar terminology is used in soil water studies. It is determined, in effect, by a balance between water potential of the solution in the vacuole of the cell (protoplast) and water in the cell walls (apoplast) and provides a mechanism by which liquid water moves into and through plants (see Figure 1). Though the cell wall is permeable to water and solutes, the membrane (or plasmalemma) surrounding the wall's inner edge is impermeable to solutes. Thus water moves into or out of the vacuole according to the difference in potential across the membrane. These differences, however, are usually so small that local equilibrium may be assumed (i.e., $\psi_{va} = \psi_{cw}$ where subscripts *va* and *cw* denote the vacuole and cell wall). Techniques are available to measure the components of ψ_{va} and ψ_{cw} separately—matric potential of the cell wall water $\psi_{m(a)}$, pressure (or turgor) potential of the solution in the vacuole, and the osmotic potential of both regions (Kramer and Boyer, 1995). The relationship between $\psi_{m(a)}$ and relative water content, RWC, is shown in Figure 6 for a *Taxus* branch suspended in a pressure chamber (McGilvary and Barnett, 1988; Kramer and Boyer, 1995). Plant water researchers express ψ in terms of bars or MPa rather than J m^{-3}, so their terminology is used here (1 bar = 0.1 MPa = 10^5 J m^{-3}). The osmotic component in the cell wall, $\psi_{s(a)}$ in Figure 6, contributes in a minor way to the total potential of the wall, which is the sum of the two components displayed. Quantity RWC is the water content of a material expressed as a percentage of the water content when the material is fully turgid (in equilibrium with pure water). This turgid state is a more convenient reference point than the dry state because it is experimentally reproducible and not as subject to error due to plant growth. Thus RWC is computed from

$$\text{RWC} = [(W_c - W_d)/(W_t - W_d)]100\% \tag{14}$$

where W_c, W_t, and W_d are the material weights in the current, turgid, and oven-dry (dried at 100°C) states. Gardner and Ehlig (1965) are among the researchers who have studied the water potential-RWC relationship. They measured RWC, ψ, ψ_s, and ψ_p of cotton, pepper, sunflower, and birdsfoot trefoil leaves and found a linear relation between osmotic potential ψ_s and RWC. The total potential ψ was not linearly related to RWC because of a change in the modulus of elasticity of the cell wall when the turgor potential ψ_p approximated +2 bars. This change in elasticity was associated with the early stages of wilting.

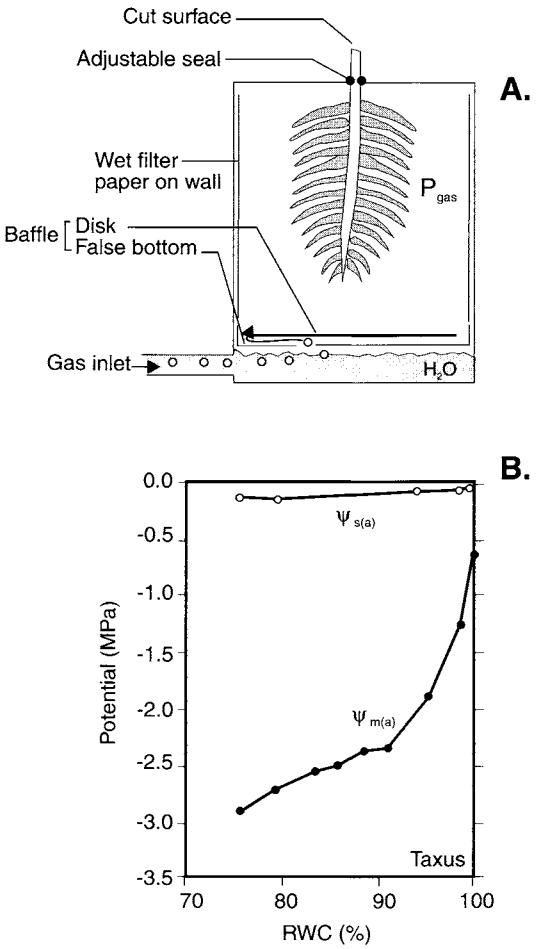

FIGURE 6 Determination of the moisture characteristic curve. (A) Pressure chamber in which incoming gas increases the pressure around a *Taxus* branch and forces xylem sap through the cut surface. The pressure is adjusted to maintain zero flow at the surface and provides an estimate of the internal tension on the apoplast. (B) Pressure chamber measurements show that water potential decreases as relative water content decreases and that a greater pull is being exerted by the leaves on water in the xylem as water content decreases. Osmotic water potential of the cell wall is given by $\psi_{s(a)}$. From Kramer and Boyer (1995).

2. Water Transport in the SPAC

The mechanisms governing transport of water through living fuels may be described by several methods. One is empirical and often used to fill knowledge gaps with information based on experimental data. In the second method, it is assumed that the water-conducting system is analogous to an electrical circuit

and requires evaluation of flow resistances in series and/or parallel connections. A third method involves solution of the differential equations governing flow in the various soil–plant–atmosphere domains and uses conductivities and diffusivities rather than resistances. The domains most conducive to analysis with differential equations are those describing soil water flow and uptake by roots. Modelers often describe flow in the whole plant using some combination of these three methods (Federer, 1979; Riha and Campbell, 1985).

a. The Ohm's Law Analogy

The driving force for water movement in transpiring plants originates in the leaves and is transmitted to the roots through the cell sap. Transpiration reduces the leaf water potential, and this disturbance is propagated through the xylem of the leaves and stem to the roots where the reduced potential induces water flow toward the roots. This process occurs when water content of the soil is high or the transpirational demand is low. On the other hand, when the soil water content is low or the transpirational demand is great, leaf water potential falls to such a low value that the leaves lose their turgor and the stomates tend to close. Thus, the leaf resistance is greatly increased, the rate of transpiration is reduced, and further loss of water is controlled by the plant and soil rather than the atmospheric conditions (Cowan, 1965). In the SPAC method of analysis, the overall movement of water may be analyzed using an analog of Ohm's law which states that the flow of current in an electrical circuit is proportional to the potential difference across the circuit. The electrical analog shown in Figure 7 is a simplified representation of the paths taken by water from its entry via the water table to its exit through the plant leaves. The xylem portion of the circuit applies to the complete vascular system—xylem in the roots, stem, and leaves. The overall process may be crudely approximated with four subprocesses: water flow from soil to roots, from roots to stem, from stem to leaves, and from leaves to the atmosphere. Figure 8 illustrates the relative magnitudes of change in water potential for each component of the SPAC. Because the change in potential from root to leaf is only a few bars, the stem sometimes is omitted from considerations of overall flow.

The SPAC is nonstationary in character because of diurnal and seasonal variation and because of periods of hydration and desiccation. To eliminate some of this complexity, plant water researchers often assume a steady state rate of transport. Though this represents considerable simplification, investigators can work with a series of steady states instead. The steady state assumption implies that a disturbance of water potential in the roots (or leaves) is propagated instantaneously throughout the plant to the leaves (or roots) and that internal changes in water content during the process are small in comparison with the magnitude of the disturbance (Cowan, 1965). Jarvis (1975) and Waring and Running (1976) argue, however, that in plants with water sources of sufficient

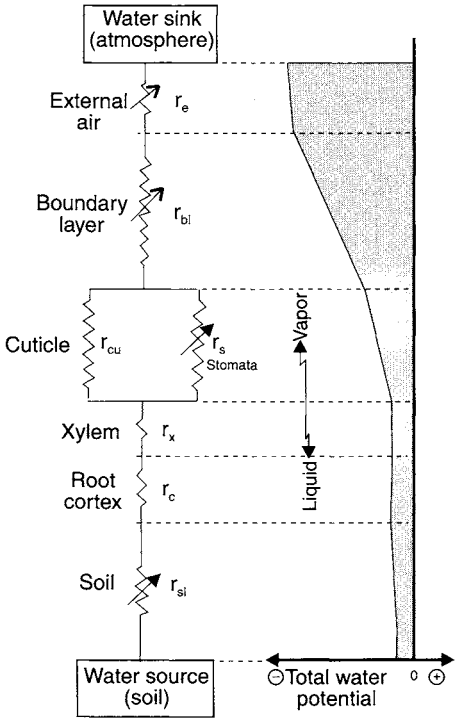

FIGURE 7 Electrical analog showing soil, root, vascular, leaf, and atmospheric flow resistances in the SPAC. Resistances r_{sl}, r_c, and r_e correspond to r_{so}, r_r, and r_a in Eq. (15); the overall resistance due to r_{cu}, r_s, and r_{bl} is represented by r_l in Eq. (15). The shaded area at the right indicates relative magnitudes of water potential for the various components. From Rose (1966).

size in the stem and branches and with radial (or horizontal) pathways to the stem xylem of low enough resistance, sufficient water may be withdrawn from these regions of storage to satisfy the transpirational demand for considerable periods. Jarvis points out that little is known about resistances to flow between these storage regions and the xylem and about the moisture characteristic of the cambium, phloem, or roots. Nevertheless, if steady state is assumed, stem resistance is omitted, and soil moisture is not limiting, the transpiration rate Q (m s^{-1}) equals the flow rate in all plant domains and

$$Q = (\psi_{so} - \psi_r)/(r_{so} + r_r) = (\psi_r - \psi_l)/(r_r + r_l) = (\psi_l - \psi_a)/(r_l + r_a) \tag{15}$$

where r (bar-s m^1) symbols denote resistances and subscripts *so*, *r*, *l*, and *a* refer to soil, root, leaf, and atmosphere. The last term in this equation is a rough approximation during the day because its value is influenced by temperature

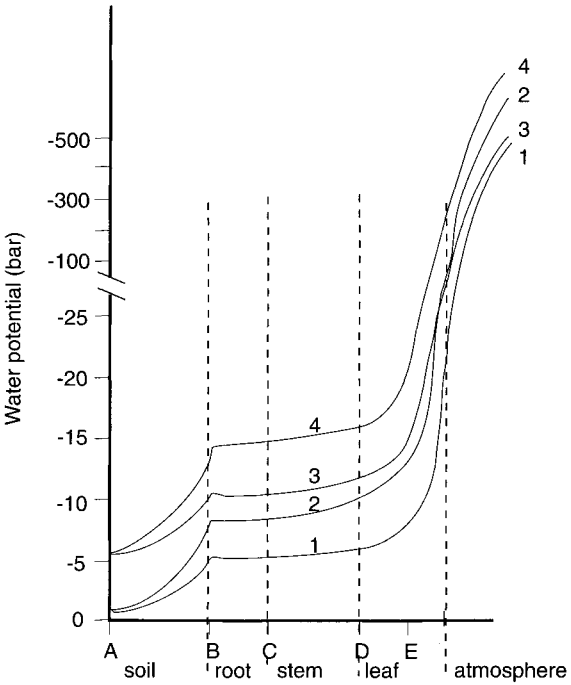

FIGURE 8 The distribution of water potential throughout a woody plant (not to scale). Curves 1 and 2 indicate extremely wet soil; curves 2 and 4 indicate a high atmospheric demand. The largest change in potential occurs in the leaf. From Hillel (1980b).

changes associated with solar radiation and periods of cloudiness. Moreover, the term often is written with differences in vapor pressure or vapor concentration replacing the water potential difference (Kramer and Boyer, 1995).

It is recognized by plant water researchers that the assumptions commonly associated with the SPAC approach, namely steady state flow and constant flow resistances, make this kind of analysis a crude approximation at best. For example, total resistances often must be evaluated by dividing the potential difference by transpiration rate Q. They are continuously changing, however, because transport can be controlled either by the soil, plant, or atmosphere. Numerous authors have studied the relative importance of r_{so} and r_r, and differences of opinion continue to exist. Results from these studies are briefly summarized by Kramer and Boyer (1995) who state "evidence seems to indicate that over a considerable range of soil water content and with average root density, root resistance exceeds soil resistance to water movement." Leaf resistance also is complicated and includes components due to liquid flow in the petiole, veins, and mesophyll cells as well as vapor diffusion through the cuticle, substomatal

cavities, and stomates (Kreith and Sellers, 1975). Root and leaf resistances from several studies are reported by Slatyer (1967) and Cowan and Milthorpe (1968).

b. *Soil–Root Models*

Movement of soil water may be described by the Richards equation which is based on mass continuity and momentum conservation as expressed by Darcy's law. Derivations of the Richards equation for saturated and unsaturated flow may be found in soil physics texts such as Hillel (1980a). If the influence of osmotic potential on soil water flow is negligible and the system is isothermal, the Richards equation for vertical flow in unsaturated soils may be written as

$$\partial\theta/\partial t = C_h(\partial h/\partial t) = \partial[\kappa_h(\partial h/\partial z) + \kappa_h]/\partial z \tag{16}$$

where θ is the volumetric soil water content, t (s) is time, h (m) is the pressure head applicable to flow caused by capillary and attractive forces, C_h (m^{-1}) is the specific water capacity given by $(\partial\theta/\partial h)$, κ_h ($m\ s^{-1}$) is the hydraulic conductivity, and z (m) is the vertical distance from the reference location. Head h is given by $P_w/\rho_w g$, where P_w ($J\ m^{-3}$ or $kg\ m^{-1}\ s^{-2}$) is the hydrostatic pressure, ρ_w ($1000\ kg\ m^{-3}$) is the density of water, and g ($9.8\ m\ s^{-2}$) is the gravitational acceleration. For horizontal flow, z must be interpreted as a horizontal distance, and the second term in the brackets is set to zero. In the case of saturated flow, conductivity κ_h may be regarded as the hydraulic conductivity of the saturated soil (a constant), and the derivative of the second term in brackets vanishes. Various empirical and theoretical relationships expressing conductivity κ_h in terms of θ or matric potential ψ_m and soil texture have been reported (Scholl, 1976; Jury *et al.*, 1991; Alessi *et al.*, 1992). Equation (16) may be expressed in terms of ψ_m ($J\ kg^{-1}$) by substituting the relationships

$$\psi_m = P_w/\rho_w = gh \qquad \text{and} \qquad \rho_w\kappa_h = g\kappa_m \tag{17}$$

into Eq. (16) to obtain

$$\rho_w(\partial\theta/\partial t) = \rho_w C_m(\partial\psi_m/\partial t) = \partial[\kappa_m(\partial\psi_m/\partial z) + g\kappa_m]/\partial z \tag{18}$$

where C_m ($s^2\ m^{-2}$) is the slope of the soil-moisture characteristic curve, or specific water capacity $(\partial\theta/\partial\psi_m)$, and conductivity κ_m (kg-s m^{-3}) differs from κ_h. Equations (16) and (18) contain no source or sink terms to account for loss or gain of soil water by the roots. Riha and Campbell (1985) added a sink term to the right side of Eq. (18) to account for absorption of such water. Their term was of the form

$$U = \rho_r(\psi_{so} - \psi_r)/(r_{so} + r_r) \tag{19}$$

where U is the root sink strength (kilogram of water absorbed per second per cubic meter of soil) and ρ_r the root density (meter of root length per cubic meter of soil). Potentials are in units of $J\ kg^{-1}$ and resistances in $m^3\ kg^{-1}\ s^{-1}$.

The uptake of soil water by roots may be modeled by two differing approaches in which the roots are treated as uniform cylinders of length L. The first method considers a single root of uniform radius surrounded by a cylindrical sheath of soil. When solute effects are neglected and equilibrium is achieved between liquid in the cell vacuole and that in the cell wall, radial transport of water into the root may be described by

$$\partial\psi_m/\partial t = D_h(\partial^2\psi_m/\partial r^2) + (D_h/r)(\partial\psi_m/\partial r) \tag{20}$$

where D_h ($m^2\ s^{-1}$) is the hydraulic diffusivity of the root tissue, r (m) is radial distance in the root, and potential ψ_m has the units J m^{-3} (Hillel, 1980b). The relationship between κ_h of Eq. (16) and D_h of Eq. (20) is

$$C_h D_h = \kappa_h \tag{21}$$

whereas Eqs. (16)–(18) may be used to write

$$C_h = gC_m \tag{22}$$

When the soil moisture contains a significant amount of solutes, differences in osmotic and matric potential between the sheath of soil surrounding the root and the root itself must be considered (Hillel, 1980a; Flowers and Yeo, 1992). The second approach is to consider the entire root system as a moisture sink which penetrates the soil to a known depth. This root zone depth may be subdivided into layers that contain different root masses per unit volume of soil. The major fault of this method is that it is based on gross averages of root density and water potential over the root zone.

c. *Leaf–Atmosphere Models*

The influence of the atmosphere on water movement in plants can be evaluated from the rate of evaporation from a free water film covering the leaf surface. This rate is referred to as the *potential rate of evaporation*, Q_0 (kg $m^{-2}\ s^{-1}$), and may be estimated from the simple "Ohm's law" equation

$$Q_0 = (\rho_{sat} - \rho_{va})/r_a \tag{23}$$

where ρ_{sat} (kg m^{-3}) is the concentration (or density) of water vapor at the leaf surface under saturated conditions and ρ_{va} the vapor concentration in the ambient air. Further discussion of Q_0 is given in Chapter 9 in this book. Resistance offered by the air to vapor diffusion from the leaf surface is r_a (s m^{-1}) and can be estimated by two methods. The first method, for continuous areas of more or less uniform vegetation, utilizes the logarithmic wind profile (see Chapter 9 in this book) and therefore considers such factors as vegetation height, zero plane displacement, and roughness length (Monteith, 1963a; Rutter, 1968). The second approach, for single leaves, makes use of boundary layer concepts and

depends on leaf size and shape and on wind speed (Kreith and Sellers, 1975). When evaporation takes place from the interior leaf surfaces, the process is referred to as *transpiration*. In this case, the resistance to vapor diffusion occurring within the leaf, r_l, should be accounted for and r_a in Eq. (23) replaced by $(r_a + r_l)$. Resistance r_l includes cuticular resistance which is in parallel with the resistance to vapor diffusion. This diffusion, or stomatal, resistance is made up of resistances originating in the mesophyll cell walls, intercellular spaces, and stomatal pores linked in series. Schönherr (1976) studied the diffusion of water through cuticular membranes and found that the water permeability of the cuticle is completely determined by waxes rather than cutin in the cuticular layer. Cuticular resistance is 10 to 100 times greater than the stomatal resistance and generally can be ignored in calculations of r_l (Kozlowski and Pallardy, 1997).

The term *evapotranspiration* refers to loss of water from the soil due to the combined water loss from plants by transpiration and from the soil surface by evaporation (see Chapter 9). When all surfaces are moist, evapotranspiration proceeds at the potential rate and depends primarily on meteorological factors. In this case, the *potential evapotranspiration*, Q_0, may be calculated by at least two different methods. The first is outlined by Kreith and Sellers (1975) and is applicable to evaporation from large areas (an ecosystem or field). Their approach requires that temperatures of the evaporating surfaces be known. The second method utilizes the Penman equation—an equation which accounts for the effect of solar radiation on the evaporation from a water surface in such a way that knowledge of surface temperatures is not required. Various forms of the equation are widely used in agricultural applications to compute Q_0. Monteith *et al.* (1965) and Monteith (1980) modified the Penman equation to describe potential evaporation from whole plants or crops over an extended area. The modified model, referred to as the Penman-Monteith equation, is discussed in Chapter 9.

According to Monteith (1980), there are only two ways to compute the actual evapotranspiration rate, Q. One method is to utilize complex models within the SPAC framework (Lemon *et al.*, 1971; Waring and Running, 1976); the second is to apply models such as the Penman-Monteith equation to the entire plant canopy. This application, which assumes that stomatal resistance is uniform throughout the canopy and that temperature, humidity, and momentum profiles are similar within and above the canopy, was questioned by Philip (1966) and Tanner (1968). Subsequent research has shown that the Penman-Monteith equation is useful when applied to well-developed crop canopies but underpredicts transpiration from sparse canopies when soils are dry and overpredicts it when soils are wet. Refinements in the equation by agricultural researchers have led to compartment schemes in which evaporation from the soil surface and transpiration from the crop canopy are treated separately (Shuttleworth and Wallace, 1985; Choudhury and Monteith, 1988). This approach has

produced better agreement with experimental measurements of transpiration because of improved modeling of soil heat and vapor fluxes (Wallace *et al.*, 1990; Tourula and Heikinheimo, 1998).

When the soil moisture or soil water potential falls below some critical value, the evapotranspiration rate falls below the potential value. Lopushinsky and Klock (1974) found that transpiration rates in several conifer seedlings began to decrease when the soil water potential fell below −2 bars (Figure 9). The transpiration rates of several pines were slower than those of fir and spruce by more than a factor of two, explaining the ability of pines to survive on fairly dry sites and the need for fir and spruce to occupy more moist sites. Lopushinsky and Klock attributed the decrease in transpiration rate to stomatal closure and noted that such closure takes place in all species when the leaf water potential ranges from about −14 to −25 bars. Brown (1977) studied the wilting process in two range grasses under controlled environmental conditions. He measured

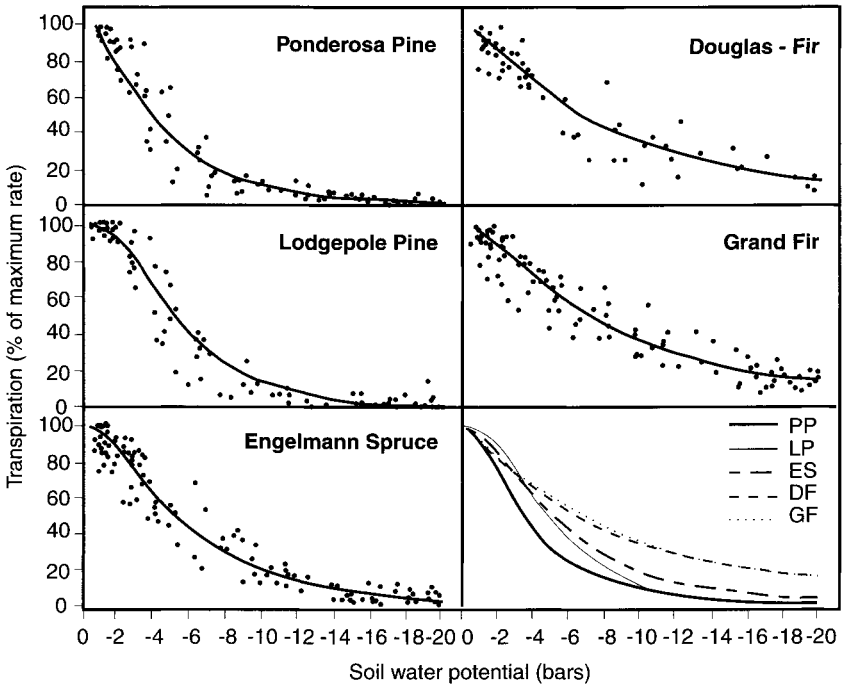

FIGURE 9 Transpiration rate as a function of soil water potential for seedlings of various conifers. Curves at the lower right represent regression equations through the experimental data. From Lopushinsky and Klock (1974). Reprinted from Forest Science (vol. 20, no. 2, p. 183) published by the Society of American Foresters, 5400 Grosvenor Lane, Bethesda, MD 20814-2198. Not for further reproduction.

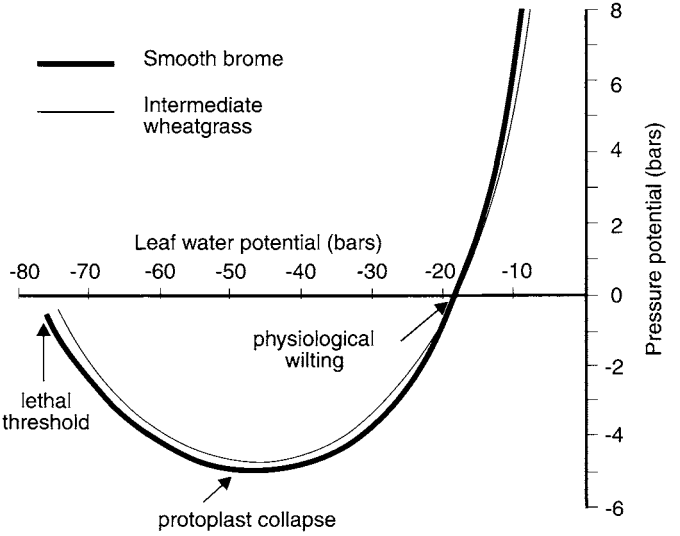

FIGURE 10 Relationship between pressure (or turgor) potential and leaf water potential for two range plants. From Brown (1977).

soil and leaf water potentials during a drying process in which the soil water potential decreased from 0 to about −65 bars. In the early stages of drying, the pressure potential (the difference between the leaf water and osmotic potentials) decreased to zero—a value labeled by Brown as the *physiological wilting point* (Figure 10). As drying continued, the pressure potential decreased to a minimum of about −5 bars (the point of *protoplast collapse*) and then increased toward zero where severe wilting occurred at a leaf water potential between −70 and −80 bars; Brown labeled this point (or range) the *lethal threshold* and associated it with the collapse of all plant cells. Brown (1977) stated that other unpublished research by him indicates the measurement techniques he used are equally applicable to trees, shrubs, forbs, and grasses growing in arid environments and that similar experiments can provide quantitative guidelines for evaluating the adaptability of range plants to dry conditions.

3. Canopy Moisture Content

The literature of forest physiology contains much information on evaporation and transpiration rates but is almost devoid of attempts to model the water content of understory and overstory canopies. It is likely that within a given fuel type there exist critical combinations of canopy moisture content, relative weights of live and dead fuel, and ambient wind speed which will permit the spread of fire in tree crowns, understory shrubs, or open grassland. The ability

to predict canopy moisture content seasonally would be a help in understanding and anticipating the initiation and spread of fire in these fuel types.

Changes in the moisture content of live fuels are poorly understood—partly because plant physiologists have studied the response of plants to environmental stress in terms of water potential rather than moisture content (Brown *et al.*, 1989). These authors also state that seasonal variation in water content is more closely related to phenological changes such as leaf growth and maturation than to environmental factors. In earlier work, Kozlowski and Clausen (1965) pointed out that changes in plant tissue moisture content can result from changes in actual water content, tissue dry weight, or both. Their phenological study of leaves from several forest trees during the 1963 growing season showed that the moisture content of all deciduous leaves studied decreased until mid-June, after which time the rate of decrease slowed and became dependent on species. This result was attributed to increases in dry weight rather than changes in the mass of water present. On the other hand, moisture content of zero-age conifer needles decreased continuously, whereas in 1-year-old needles it increased until about mid-July and then became relatively constant. In this case, the dry weight changes were attributed to carbohydrate translocation into new needles and out of the older ones. Little (1970) conducted a year-long study of water, sugar, starch, and crude fat content in juvenile balsam fir needles. In contrast with the results of Kozlowski and Clausen (1965), he found that seasonal fluctuations in moisture content generally were caused by changes in actual water content rather than by dry weight changes. Little pointed out, however, that changes in moisture content due to dry weight changes increase with increasing age, and that increased carbohydrates may not have accounted for the total change in dry weight of his study—as they might have in the maturing balsam fir needles of the Kozlowski and Clausen study. Research on Engelmann spruce needles conducted by Gary (1971) showed that moisture contents were determined primarily by dry weight changes and that differences between needles from north and south slopes were small. Chrosciewicz (1986) sampled the foliar moisture content of several Canadian conifers in central Alberta. His sampling procedure was designed to minimize variation due to the diurnal cycle and sample location within the canopy. Figure 11 shows some of his results for new and old (needles 1, 2, and 3+ years old) foliage measured during 1974. The flushing of new foliage coincides with the moisture content minimum in the old foliage. Moisture content of the new foliage approaches that of the old in September.

In a study extending from January to October 1971, Hough (1973) measured extractive content, phosphorus content, and moisture content of old and new needles to determine their effects on the flammability of natural sand pine stands. A sharp rise in moisture content of new needles up to 10 months in age coincided with the initiation of new growth, whereas ether-soluble extractives

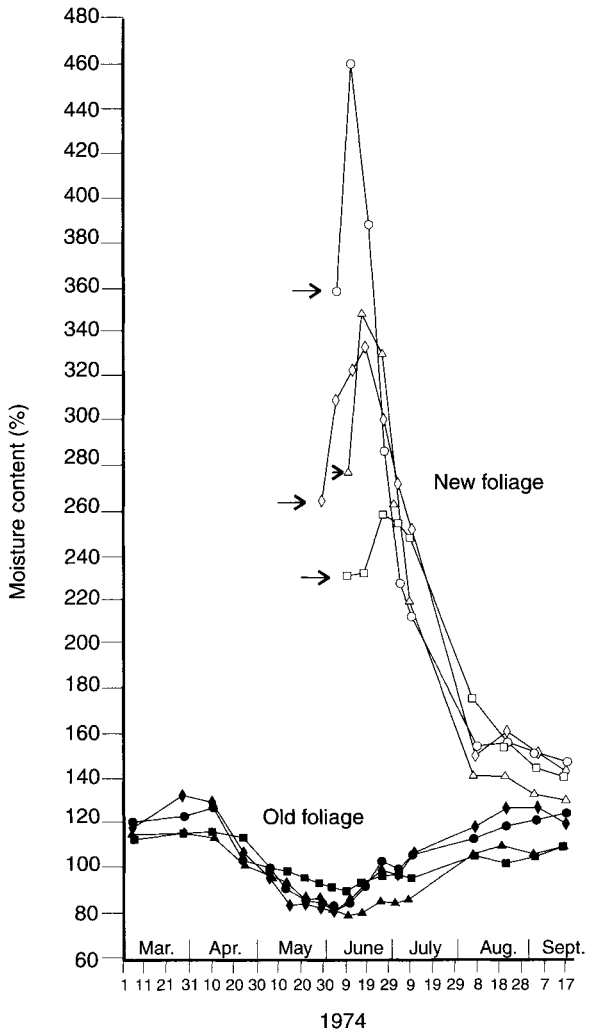

FIGURE 11 Seasonal moisture content variation in new and combined old foliage (1, 2, and 3+ years old) of four Canadian species. Right-pointing arrows indicate the start of flushing of new foliage. With the arrows as reference points, the species from top to bottom of the figure are white spruce, black spruce, balsam fir, and jack pine. From Chrosciewicz (1986).

of new and old (9–18 months in age) needles peaked in late February and then decreased until June. Phosphorus content of new needles decreased until March and then peaked in late May, while that of the old needles decreased until April and then slowly increased. Hough concluded that both weather and fuel variables affect fire occurrence in stands of sand pine in Florida and that crown fires

would be most likely to occur in late February and early March. He stated that the severity, or intensity, of wildfires is not reduced until the new needles, with their high moisture content and low extractive content, make up most of the crown.

One naturally would expect understory vegetation to show patterns of variation in moisture, mineral, and extractive content similar to those in tree crowns (Hough, 1973), and the results of numerous experimental studies have shown this to be so. Fire researchers have documented the moisture content of chaparral and brush fuels in southern California for many years. Countryman (1974), for example, reported field data on the variation in moisture content of manzanita and snowbrush (Figure 12). New growth in both species typically begins in early June with moisture contents of about 200% of the fuel ovendry weight. The moisture content of old foliage increases more slowly, and both species reach a minimum level in September. Countryman stated that the percent of total fuel made up of living material usually ranges from 65 to 85% and that fire behavior in the chaparral types depends on both live fuel moisture content and relative amount of dead fuel present. According to Blackmarr and Flanner (1975), the understory shrubs growing on organic soil in the pocosin areas of eastern North Carolina cause a severe fire hazard during periods of drought. These authors sampled the moisture content of six shrub species native to the area for a 22-month period. Their 1964 and 1965 data for deciduous and evergreen species showed that all parts of the evergreen foliage were consistently drier (ranging from 250 to 100% during the summer) than those of the deciduous species (350 to 150%), tending to make them more flammable. In earlier work, Blackmarr and Flanner (1968) measured the diurnal moisture content variation in four North Carolina pocosin species over a 36-hour period during June 1965 and found differences ranging from about 25 to 40% moisture content.

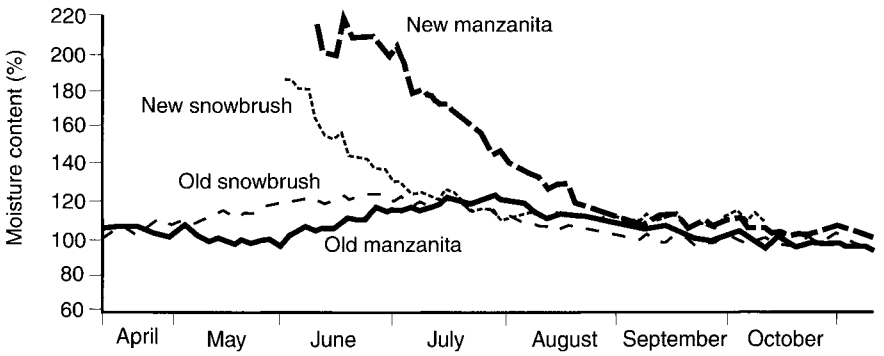

FIGURE 12 General trend of seasonal moisture content variation in two chaparral fuels in southern California. From Countryman (1974).

The moisture content of live fuels in open grasslands generally follows patterns similar to those of the understory shrub and crown fuels discussed earlier, but it also differs in some respects. These patterns are determined primarily by weather. The annual grasses usually have shallow root systems and therefore depend strongly on moisture availability near the soil surface for their growth. In the spring, these green grasses can attain fractional moisture content values larger than 3.5. As hotter weather approaches, the growth of annuals (roughly from May to July in the United States) is shortened by the absence of rainfall. The plants mature, produce seed, and then begin to cure (or dry). Their rate of curing depends on soil moisture and rainfall, resulting in curing times that may vary from three to eight weeks. As the plants flower and produce seed, the color of their various parts turns from green to yellow (or other colors such as purple, depending on species). According to Luke and McArthur (1978), this process begins in the annuals of Australia when the moisture content fraction has decreased to about 1.75. As the moisture fraction drops below 1.0, yellowing has affected about 30% of the plant surface, and the grass is said to be 30% cured; at a moisture fraction of about 0.5, the grass is 60% cured and has reached a state of dryness such that it cannot recover its moisture regardless of the amount of additional rainfall. At moisture fractions below 0.3, annuals are close to fully cured and become dead fuel now subject to changes in atmospheric relative humidity and temperature. The perennial grasses exhibit a similar, but longer, curing period (from May to September in the United States) because they have root systems that penetrate more deeply into the soil than those of annuals; this makes them less sensitive to short-term weather and surface soil moisture. In warm and humid climates, some parts of perennials cure and die whereas other parts remain alive but in a dormant state (Schroeder and Buck, 1970). In the United States, Brown (1977) reported water potential relationships he observed during the wilting of two range grasses (see Section III.C.2.c); Brown *et al.* (1989) measured the moisture content of perennial grasses under aspen stands in Wyoming. The latter authors noted a change in color of the green vegetation at a moisture fraction of about 1.0 (corresponding to 30% curing of Australian annuals) and found that these grasses green up and increase in moisture content in response to rainfalls greater than 6 mm. Similarly, Luke and McArthur (1978) reported a delay in the curing of Australian perennials due to 30 mm of rain. The moisture content of grassland fuels in Australia has been related to the Keetch-Byram Drought Index (see Section IV for several references on drought). Luke and McArthur (1978) state that Australian annuals are fully cured when the Keetch-Byram index exceeds 200 and that perennials are cured when the index is close to 600. In studies conducted in the United States (northeastern California), Olson (1980) observed that the foliar moisture content of bluebunch wheatgrass (a perennial) decreased exponentially as the Keetch-Byram index increased.

While the need for models that predict moisture content change in the cano-

pies of grass or understory/overstory vegetation is generally recognized, the complexity of the task may have precluded all attempts to develop a reasonably complete physics- and physiology-based model (Tunstall, 1991). The required model should include compartments treating such topics as soil water transport to roots and directly to the atmosphere, water takeup by roots, water rise in the main stem, growth of roots, stem, and foliage as determined by photosynthesis and respiration, storage and translocation of water and food, water potential interactions, water vapor diffusion through leaves and into the atmosphere, and senescence (the process of wilting and dying). A practical solution to the problem may be achievable if we can eventually identify and model a few key controlling processes (Howard, 1978); alternatively, perhaps we can successfully modify existing models of growth and transpiration in conifers and understory vegetation to obtain reasonable predictions of canopy moisture content (Running, 1978, 1984a, 1984b).

D. Dead Fuel Moisture

The moisture content of dead forest fuels in the hygroscopic range is of considerable interest to fire managers. The equilibrium moisture content is useful in laboratory studies in which classical diffusion theory describes moisture change driven by step changes in the fuel's environment. More recently, equilibrium concepts have been combined with diffusion theory to develop new methods for estimating the moisture transport properties of fuels under field conditions.

1. Equilibrium Moisture Content

The fractional equilibrium moisture content M_e represents the constant value of M attained by dead forest fuels when they are exposed for an extended period in air of constant relative humidity and temperature and in which changes due to variability in wind, solar radiation, and barometric pressure are small. In laboratory experiments, equilibrium values of fuel moisture content depend on whether that state is attained following adsorption or desorption because of various mechanical and environmental factors that result in sorption hysteresis. The effects of hysteresis are not apparent in field studies because of a continuously changing environment. Models that describe the equilibrium state in fuels and soils over the entire range in relative humidity eventually will simplify the description of capillary and sorption processes in composite layers of soil, duff, and litter.

a. Adsorption and Desorption

When wood and foliage reach equilibrium at various values of H and constant T, the resulting M_e values, plotted versus H, form a sigmoid curve charac-

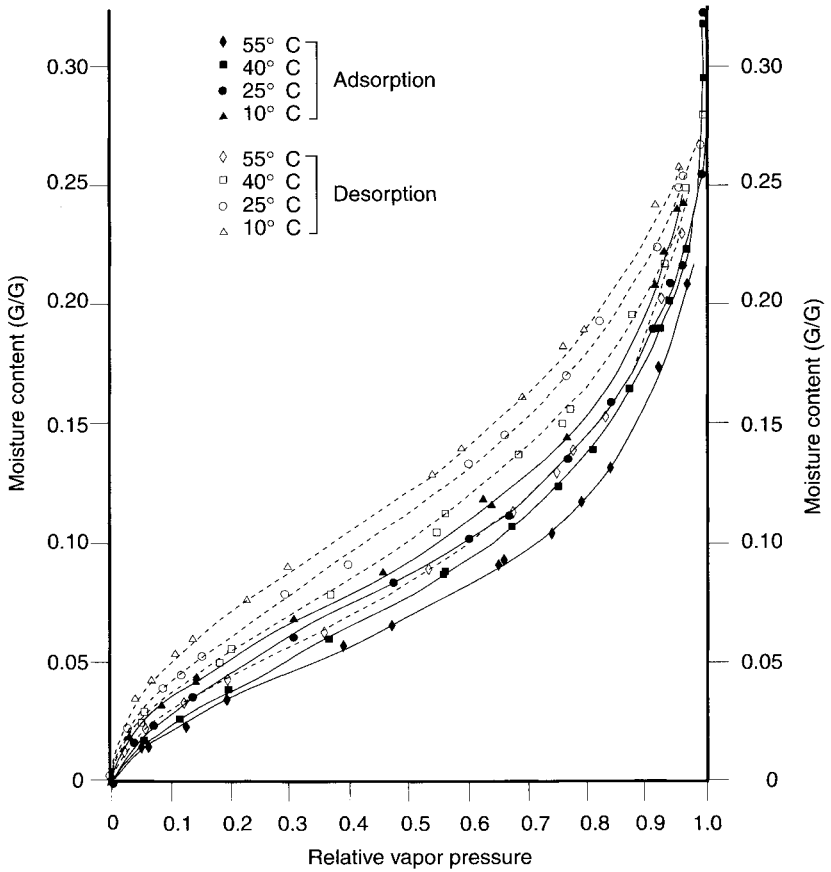

FIGURE 13 Sorption data for klinki pine wood at four temperatures. Note crossing of the 40°C adsorption isotherm over the 25°C curve at a relative vapor pressure of about 0.95. From Kelsey (1957). Reproduced by permission of CSIRO Australia.

teristic of most natural materials. If the successive H values increase, M_e increases, and the process is referred to as *adsorption;* when the H values decrease, *desorption* is occurring. The resulting curves are called adsorption and desorption *isotherms,* and the combined processes are often referred to as sorption. Figure 13 illustrates these isotherms for klinki pine wood at temperatures from 10 to 55°C. The region in H from 0 to about 0.2 is considered one in which most of the water in the wood is held by hydrogen bonding in a single layer. The slightly curvilinear region from 0.2 to about 0.9 involves water held in multiple layers within the cell walls but possibly also includes a small amount of capillary condensed water in the finest cell wall capillaries as H approaches 0.9.

Most of this water adds its volume to that of the cell walls and the composite is best thought of as a solid solution (water dissolved in cell wall substance). Because of swelling, the internal area available for adsorption due to forming cellulose-water bonds or water bridges between hydroxyl groups is about 1000 times greater than the area that would be available if water did not swell wood. True capillary condensation takes place for H between 0.9 and 0.95, but these values are rarely exceeded in commonly used experimental methods of measurement. Specialized measurements extending H to 0.999+ have been made on wood and wood pulp using the tension plate, pressure plate, pressure membrane, or nonsolvent water methods (Cloutier and Fortin, 1991; Zhang and Peralta, 1999).

The effect of previous history on sorption for a given temperature is evident in Figure 13 as the difference in M_e values for adsorption and desorption at constant H, referred to as *sorption hysteresis*. The two most generally accepted explanations of hysteresis are based on the availability of sorption sites in the material and on the rheological properties of wood. In the sorption site theory (Urqhart, 1960), it is supposed that during the initial desorption from the green condition, all available hydroxyl groups will have water molecules attached to them. As these molecules leave the sites and shrinkage occurs, many of the sites become mutually satisfied through formation of cellulose–cellulose bonds and a certain amount of rearrangement of the cellulose takes place; some unsatisfied hydroxyl groups remain, however, even when H is zero. Now as H is increased during adsorption, water molecules are adsorbed on these remaining sites, and nearly all sites will have one or more attached molecules, reducing the attraction for additional molecules. Thus a greater H is required during adsorption to attach the same number of water molecules (or achieve the same M_e value) as in desorption. This mechanistic theory of Urqhart (1960) remains, for many researchers, the most reasonable explanation of hysteresis.

Research has not yet shown whether Urqhart's theory conflicts with the thermodynamic arguments proposed by Barkas (1949) to explain hysteresis in wood based on rheological properties, but it seems likely that the two explanations will prove to be compatible. The rheological theory states that hysteresis appears because gels such as wood are not perfectly elastic and hydrostatic stresses caused by resistance to shrinking or swelling of the cell wall introduce M_e values differing from the stress-free (or perfectly elastic) value. On the one hand, fiber direction differences in the cell wall (Figure 3A) induce tension into wood undergoing desorption, causing a larger M_e than if the wood were stress free. On the other hand, interfibrillar bonding causes wood that is swelling during adsorption to be in compression, resulting in a smaller M_e than if the wood were stress free. Barkas (1949) shows that the area enclosed by a constant-temperature hysteresis loop (as in Figure 13) represents the net work loss during the entire sorption cycle. For spruce wood, Barkas calculates that this area

equals 17% of the total work of desorption. According to Skaar (1988), this means that the ratio of M_e values for adsorption and desorption in spruce should come to 0.83 (1 − 0.17 = 0.83) when averaged over the entire range in H. This overall *hysteresis ratio* averages about 0.83 for both softwoods and hardwoods (Skaar, 1988). For woody fuels, the hysteresis ratio for specific values of H generally ranges from 0.75 to 0.85 over the entire range in H from 0 to 1 (Stamm, 1964). These discrete ratios for some foliage fuels are more sensitive to H, as indicated by values ranging from 0.61 to 0.86 (Nelson, 1984).

The immediate effect of temperature on water vapor sorption by forest fuels is a reduced value of M_e as T increases. The reduction is due to the strong dependence of saturation vapor pressure on T and the resulting tendency for more water molecules to leave their sorption sites as T increases but H remains constant. This reversible effect is illustrated in the desorption data of Figure 13. Van Wagner (1972b) reported a decrease in M_e averaging about 0.024 per 10°C increase for desorption in aspen and pine leaf litter and about 0.018 in aspen wood splints. On the other hand, King and Linton (1963) and Anderson *et al.* (1978) reported a decrease of about 0.01 per 10°C increase for sorption in assorted natural fuels and ponderosa pine needles, respectively. At high values of T and H, a second temperature effect, an irreversible reduction in hygroscopicity, occurs when exposure times are long. The wood becomes discolored, and the most hygroscopic component, the hemicellulose, decomposes first followed by the pure cellulose. A still different effect at the higher values of H is that the adsorption isotherms of wood and cellulosic materials at temperatures exceeding about 40°C may cross those for lower temperatures. The effect is present in Figure 13 in which the 40°C adsorption isotherm crosses the 25°C isotherm at about $H = 0.95$. Though the 55°C isotherm does not extend to sufficiently high H values to indicate crossing at that temperature, the data suggest that crossing can occur in once-dried wood at about 40°C. Unfortunately, there exist no extensive laboratory data illustrating crossover in wood. The phenomenon has been observed in American Uplands cotton (Urquhart, 1960) in which the 70 and 90°C isotherms crossed those for lower temperatures when H exceeded 0.85. Both Urquhart (1960) and Stamm (1964) attribute the crossover effect in cotton to plasticization of the cellulose fibers; the resulting molecular rearrangement relieves drying stresses introduced when the cotton was first dried, making new sites available for adsorption. Figure 13 also shows that for $H = 0.5$ the magnitude of hysteresis in klinki pine wood decreases by a factor of nearly 2 as T increases from 10 to 55°C; Skaar (1988) refers to German research indicating that sorption hysteresis in European spruce wood disappears between 75 and 100°C. In a study of water vapor sorption by conifer and hardwood litter, Van Wagner (1972b) noted that hysteresis decreased by a factor of about 2.5 at "medium" values of H when T increased from 16 to 49°C.

Sorption of water vapor by forest fuels in the field is strongly affected by en-

vironmental variables, and even the finest fuels rarely achieve equilibrium with the continuously changing H and T values of the ambient air. The effects of H and T on sorption are modified, however, by wind and by daytime solar radiation and nighttime longwave radiation to the sky. These factors cause H and T in the air immediately adjacent to the fuel surface to differ from their ambient values. Thus M_e for a given fuel is a continuously changing value that would be obtained if the fuel were exposed for a hypothetically infinite time to these different values of "fuel" temperature and fractional relative humidity, T_f and H_f. One way to estimate M_e is to assume that T_f and H_f are the same as T and H. In this case, approximating T_f with T might be acceptably accurate only if the fuel were beneath a dense forest canopy, and even then, perhaps only at night. The second, and more appropriate, way to obtain M_e under field conditions should utilize measurements or models to evaluate T_f and H_f. Byram and Jemison (1943) collected data on fuel temperature, air temperature and humidity, wind, and fuel moisture content in an artificial sun apparatus in which fuels (hardwood leaf litter or basswood slats) were exposed to simulated solar radiation and wind generated by light bulbs and fans. The data were used to develop constants in a mathematical expression describing the effects of radiation and convection on the temperature difference $(T_f - T)$. Byram and Jemison then used this difference to compute the ratio H_f/H by assuming that vapor pressures in the fuel and air were equal. Values of M_e were determined by applying T_f and H_f to tabulated equilibrium sorption data for wood. These figures were in good agreement with measured M_e, substantially verifying the substitution of T_f and H_f for T and H. Byram and Jemison also studied experimentally the effect of wind and solar radiation on M_e obtained following the drying of basswood slats containing free water. They found that M_e for irradiated slats was larger when ventilated than when wind was absent and attributed the difference to higher H_f and smaller T_f values caused by the cooling action of the wind. Van Wagner (1969b) repeated the field experiments of Byram and Jemison in a laboratory setting to test the form of their equation for T_f. He observed similar effects of wind and radiation on T_f for jack pine and aspen litter fuels, but the mathematical form of his equation was slightly different. Viney (1991) critiqued the Byram and Jemison (1943) approach and noted omission of the effects of longwave radiation and vertical gradients in vapor pressure on T_f and H_f.

b. Sorption Models

The study of sorption systems involving various solid–gas interactions has led to identification of five types of sorption (Stamm, 1964). Type I sorption occurs on all solids in a single molecular layer at temperatures above the critical temperature of the gas. Types II and III take place in swelling solids and exhibit sorption in multiple layers. In Type II, large quantities of heat are liberated due

to strong interaction between the solid and the gas; in Type III, this interaction is weak. Types IV and V are special cases of Types II and III and describe sorption in solids with very fine pores that become filled before the saturation vapor pressure is reached. Researchers in the fields of wood products, textile manufacturing, leather processing, and food technology have found that water vapor sorption isotherms for their respective materials follow Type II sorption. One of the first isotherms derived for Type II adsorption was the Brunauer-Emmett-Teller (BET) isotherm—a model that did not represent water takeup in wood very well but spawned other theories that describe water takeup over the entire range in H. Prior to the BET theory, however, the Bradley isotherm had been developed on the basis of reduced dipole attraction between successive layers of adsorbed water vapor molecules. Anderson and McCarthy (1963) derived an equation similar in form to the Bradley isotherm. Their semiempirical theory was based on experimental data that suggested the natural logarithm of the partial molal enthalpy of adsorption is linearly related to M_e; it successfully described water vapor sorption data in silk, nylon, and cotton fibers over a range in H from about 0.1 to 0.85. A detailed discussion of sorption theories is beyond the scope of this chapter; the reader may consult the summary in Skaar (1988).

Despite its apparent success, the Anderson-McCarthy sorption equation must be regarded as approximate because it uses the highly improbable assumption that the entropy change of the adsorbed water always is zero. In an alternative approach, Nelson (1984) reported that for sorption in forest fuels the natural logarithm of the change in Gibbs free energy, ln ΔG, is linearly related to M_e over most of the hygroscopic range according to

$$\ln \Delta G = A + BM_e = \ln \Delta G_d[1 - (M_e/M_{est})] \tag{24}$$

where ΔG_d (J kg^{-1}) is the limiting value of ΔG as M_e and H approach zero, and A and B are constants. Quantity M_{est} is an estimate of the fiber saturation point M_{fsp} under desorption conditions; for adsorption, M_{est} approximates the αM_{fsp} product, where α is the hysteresis ratio. The decrease in Gibbs free energy when pure liquid water is adsorbed by forest fuels is defined as the difference between the Gibbs free energy of water vapor in equilibrium with pure liquid water (the reference state) and the energy of water in the adsorbed state. Thus at constant T,

$$\Delta G = G_0 - G = \int_p^{p_0} V_v dp = -\int_{p_0}^{p} (RT/M_w) dp/p = -(RT/M_w) \ln H \tag{25}$$

where G_0 refers to the reference state, V_v is the specific volume of water vapor at ambient temperature T, R is the universal gas constant (8.32 J mol^{-1} K^{-1}), and M_w is the molecular weight of water (0.018 kg mol^{-1}). Vapor pressures in

the adsorbed and reference states are p and p_0, respectively, and the vapor is assumed to be an ideal gas. The sorption isotherm may be written by combining Eqs. (24) and (25) to give

$$M_e = \{\ln[(RT/M_w)(-\ln H)] - A\}/B \tag{26}$$

in which B is a negative number. Clearly, as H approaches 0, M_e approaches negative infinity, and as H approaches 1, M_e approaches infinity. Increasingly erroneous values of M_e are predicted as H decreases below about 0.1 or increases beyond 0.85. The model in Eq. (26) was used to describe water vapor sorption in forest fuels, including hardwood leaves, pine needles, and wiregrass (Nelson, 1984). The maximum difference between measured and modeled M_e values was about 0.02.

In a comprehensive study, Anderson (1990b) utilized Eq. (26) to describe sorption in recently cast and weathered (over one winter) litter collected from sites in northern Idaho and western Montana. The twofold purpose of the research was (1) to test applicability of the model for forest fuels and (2) to determine whether the model would aid in separation of the litter types studied into groups with similar M_e values. A total of 94 runs involving adsorption and desorption in fresh and weathered fuels and spanning a temperature range from 278 to 322 K was made. Anderson found that a minimum of 89% of the variation in ln ΔG of Eq. (24) was explained by variation in M_e. He identified four distinct fuel groups for recently cast fuels on the basis of ± 0.02-wide bands within the M_e data; there were only a few species changes within the basic groups for the weathered litter. In order of increasing M_e, the four groups are referred to as grasses, spruce and fir needles, pine and cedar needles, and aspen and larch foliage. Encouraged by results of the study, Anderson stated that only a few fuel groups were needed to describe changes in M_e for a large assortment of fuel litters. The constants A and B of Eq. (26), documented in his Table 2, provide a wealth of information for researchers interested in modeling equilibrium relationships or water transport below M_{fsp} in foliage fuels.

c. *Complete Sorption Isotherms for Wood and Soil*

The isotherms of the previous section involve sorption of water below M_{fsp} and, therefore, are strictly applicable for $H < 0.9$. Soil and plant researchers have been interested in the region $H > 0.9$ for many years, but only a few wood and paper researchers have reported on sorption in this region since the mid-1960s. What is referred to here as a *complete isotherm* involves a range in M_e from the ovendry to water-saturated condition. Only when wood is totally saturated will $H = 1$ and water potential $\psi = 0$. For abiotic materials such as wood

and soil, ψ must be interpreted as the sum of the osmotic and matric potentials because both of them cause a reduction of the vapor pressure of liquid water. Moreover, they are not easily separated experimentally (Cloutier and Fortin, 1991). Thus Eqs. (3) and (25) may be combined to give

$$\psi = \rho_w(\mu - \mu_0)/M_w = -\rho_w \Delta G = (\rho_w RT/M_w) \ln H \tag{27}$$

so that water potential is negative, as it should be if the vapor pressure is reduced below that of the reference state. Capillary water within and between fuel or soil particles is assumed to form hemispherical menisci in which the liquid–gas interface separates liquid pressure P_w and gas pressure P_g. These pressures are related to the principal radii of curvature of the air–water interface, r_1 and r_2, and the surface tension of water, γ, by the equation

$$P_w - P_g = -\gamma[(1/r_1) + (1/r_2)] = -2\gamma/r = \psi \tag{28}$$

when $r_1 = r_2 = r$ and the wetting angle of water on the solid material is assumed to equal zero. Figure 14 shows data relating M_e to ψ for western hemlock specimens 10 mm thick in the longitudinal direction at $T = 21°C$. The data at high M_e values were obtained in 1979 by Fortin (cited by Cloutier and Fortin, 1991) with the tension plate and pressure plate methods; the dashed lines represent data obtained with saturated salt solutions in the hygroscopic

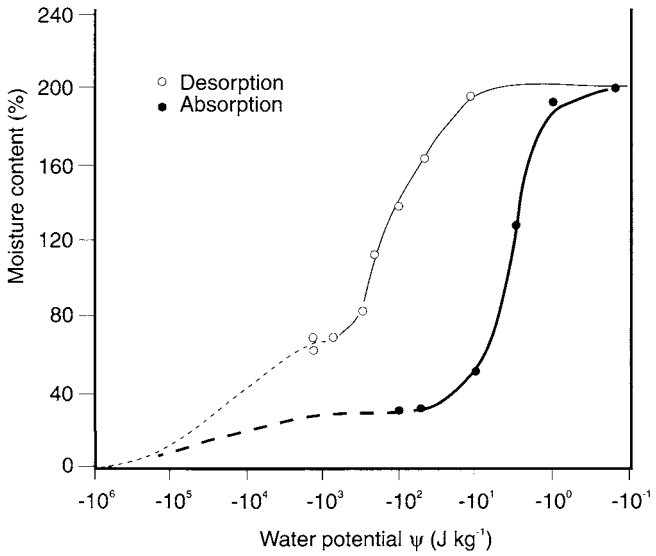

FIGURE 14 Moisture content of western hemlock sapwood as a function of water potential over the range from the nearly ovendry to saturated condition. Temperature is 21°C. From Cloutier and Fortin (1991).

region using Eq. (27). For this figure, ψ has units J kg^{-1}, but these are easily changed to J m^{-3} because the density of water is 1000 kg m^{-3}. The hysteresis prominent in the data of Figure 14 is attributed by Cloutier and Fortin (1991) to the "ink-bottle effect" in which water gain or loss is dependent on the distribution of capillary sizes and shapes. In wood, evaporation to a given water content is determined by radii of the smaller channels (pit membrane pores connecting cell cavities), whereas condensation approaching the same water content depends on the radii of the larger pores (the cell cavities). Thus Eqs. (27) and (28) indicate that both ψ and H are smaller for desorption than absorption at constant water content, in qualitative agreement with Figure 14.

In earlier years, soil water equilibrium relationships were expressed in terms of matric suction (a pressure difference across a differentially permeable membrane) and moisture content. Campbell *et al.* (1993) have simplified the presentation of such data by developing a complete isotherm similar in form to Eq. (26). The isotherm of Campbell *et al.*, given by their Eq. (4), may be written (using symbols of this chapter for water activity and equilibrium water content) as

$$H = \exp\{-(M_w/RT) \exp[(1 - M_e/M_1) \ln(-\psi_d)]\} \tag{29}$$

where M_1 is the extrapolated value of M_e when $\psi = -1$ J kg^{-1} and ψ_d is the water potential of ovendry soil, evaluated as the constant -10^6 J kg^{-1}. Because the quantities $-\psi_d$ and M_1 of Campbell *et al.* are equivalent to ΔG_0 and M_{est} of Eq. (24), it is easy to show using Eqs. (27) that Eqs. (24) and (29) are identical in form. In addition to simplifying the mathematical modeling of soil drying, Eq. (29) may be used with Eq. (26) to characterize moisture equilibrium between mineral soil and the adjacent duff and litter layers. This possibility was pointed out by Siau (1995).

2. Laboratory Studies

The transport of moisture through a fuel particle is determined by the relative magnitudes of internal and external transfer of water as determined by particle properties and ambient conditions. However, in highly impermeable wood or in a composite fuel layer (litter, duff, and mineral soil, for example), internal evaporation and/or infiltration (gravitational flow of liquid water) also may take place. These processes initially were studied with diffusion theory, but advances in describing the flow of liquid water in wood and granular materials by capillarity now provide more realistic analyses of moisture transport.

a. Transport Mechanisms

The mechanisms by which water moves through the interior of dead forest fuel particles and layers are capillarity, diffusion, and infiltration. The latter process is described in soil physics texts such as Hillel (1980b). When gravitational

forces have ceased to operate, liquid water is brought to the particle or layer surface where it evaporates into the atmosphere; water in vapor form either condenses on a cell wall or continues to diffuse until it passes into the environmental air. Spolek and Plumb (1980) stated that the permeability of wood to the gas phase can be neglected because many of the bordered pits become aspirated by surface tension forces associated with liquid flow. Thus for materials with fine capillaries, Darcy's law [Eq. (9)] is used to compute flows of liquid, and the flux of vapor [Eq. (11)] may be regarded as due to diffusion only. In analyzing liquid flow, Spolek and Plumb (1981) defined the local liquid saturation, S, as

$$S = (m - m_{fsp})/(m_{max} - m_{fsp}) \tag{30}$$

where m denotes local values of the moisture fraction and m_{max} is the maximum possible m calculated from the wood density (Stamm, 1964). Clearly, S can range from 0 to 1 when $m \geq m_{fsp}$. If the fuel temperature is below 60°C and the total pressure P_T in Eq. (9) is considered constant, the liquid water flux J_w may be expressed in terms of S or m by establishing a relationship between capillary pressure P_c [see Eq. (12)] and S. Spolek and Plumb (1980) reported a set of equations for this purpose based on the capillary flow model of Comstock (1970). In later work, Spolek and Plumb (1981) presented the empirical equation

$$P_c = 1240S^{-0.61} \tag{31}$$

where P_c has the units J m^{-3}. These authors implied that local values of S can replace the volume-averaged values they measured at several positions within each of their wood samples, so S is used in Eq. (31). When this equation is combined with Eq. (9) and P_T is assumed constant, the flux of liquid becomes

$$J_w = -756(K_w/\eta_w)S^{-1.61}(\partial S/\partial x) \tag{32}$$

where J_w is on a volume of whole wood basis. Combination of the relation $\rho_w \phi_w = \rho_f(m - m_{fsp}) = \rho_f(m_{max} - m_{fsp})S$ with Eqs. (5) and (32) leads to the liquid water transport equation

$$\rho_f(m_{max} - m_{fsp})\partial S/\partial t = 756(K_w/\eta_w)\partial[S^{-1.61}(\partial S/\partial x)]/\partial x - w_w \tag{33}$$

where ρ_f is density of the dry fuel.

The diffusion mechanism involves bound water and water vapor. Local diffusion of bound water when $m < m_{fsp}$ is due primarily to surface diffusion—a process in which water molecules hop from one sorption site to another in two dimensions. This diffusion is driven by a gradient in spreading pressure, P_b, and is described by Eq. (10). Practical use of Eq. (10), however, requires a known relationship between m and P_b (e.g., Nelson, 1986a). In addition, water vapor traverses the cell cavities by diffusion. The ideal gas law may be used to express Eq. (11) (with the diffusion term only) in terms of a gradient in vapor pressure.

Thus combined bound water and water vapor diffusion consists primarily of a series of steps involving evaporation from a cell wall, vapor diffusion across the adjacent cell cavity, condensation on the opposite wall, and bound water diffusion through the wall. Stamm and Nelson (1961) found from combined diffusion calculations based on an electrical conductance analogy utilizing premeasured wood structural features that 86% of the total flow in softwoods with a specific gravity of 0.4 drying at 50°C is due to this mechanism. Much of the remaining flow is continuous vapor diffusion through the cavities and pit membrane pores. Rather than solve separate mass conservation equations for bound water and water vapor, other modelers (Choong, 1965; Gong and Plumb, 1994) have used a combined diffusivity in place of D_b in Eq. (10). When this modified equation is substituted into Eq. (5), the diffusivity in the resulting diffusion equation becomes a complex function of fuel internal structure, air (or fuel) temperature, and local moisture fraction m. Numerically based prediction models combining capillary and diffusive mechanisms with energy conservation and volume averaging have been used to simulate the drying of wood (Spolek and Plumb, 1980; Perre *et al.*, 1990; Gong and Plumb, 1994).

In some types of fuel, evaporation takes place within the material rather than on the surface. This retreating-surface mechanism occurs in thick layers of porous materials (Nissan and Kaye, 1957) and in wood in which the free water is relatively immobile due to little or no continuous void structure (Stamm, 1964). Nissan *et al.* (1959) analyzed this phenomenon in thick textiles wound on bobbins that were dried in a wind tunnel at about 50°C. The temperature-time data for wool in Figure 15 indicate a temperature plateau at 30°C, about 5°C greater than the wet-bulb temperature. This increase is due to a balance between heat arriving at the internal surface of evaporation and heat used to evaporate free water and produce outward vapor diffusion. Nissan *et al.* called this intermediate temperature the *pseudo-wet-bulb temperature* and described its calculation. The two major assumptions are that (1) temperature and vapor concentration gradients in the outer dry layer are similar and (2) all incoming heat is used to evaporate free water at the retreating free water surface. The heat balance equation derived by Nissan *et al.* is

$$\begin{aligned} k(\Theta - \Theta_{pwb}) &= (\varepsilon D_v)_{pwb}\lambda_{pwb}(\rho_{pwb} - \rho) \\ &= 0.00216(\varepsilon D_v)_{pwb}\lambda_{pwb}[(p_{pwb}/T_{pwb}) - (p/T)] \end{aligned} \tag{34}$$

where subscript *pwb* denotes evaluation at the pseudo-wet-bulb temperature, absence of a subscript indicates ambient air values, k (J m^{-1}s^{-1}K^{-1}) is thermal conductivity of the material, Θ and T are Celsius and Kelvin temperatures, ρ (kg m^{-3}) is vapor concentration, λ (J kg^{-1}) is the latent heat of evaporation, and p (J m^{-3}) the vapor pressure. With this equation and a generalization of Eq. (43), it can be shown that response time τ should vary directly with d^2 and

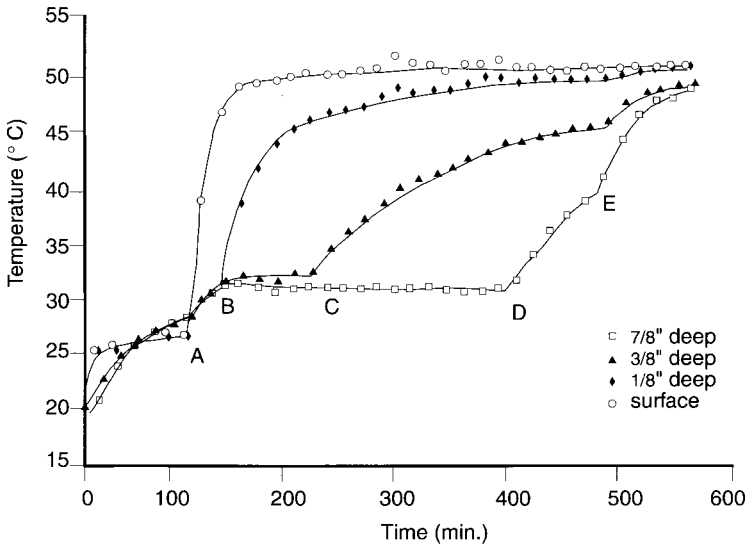

FIGURE 15 Temperature variation with time at various depths for a thick porous wool bobbin dried at 50.9°C and an airspeed of 4.35 m s^{-1}. Point A corresponds to the end of the constant-rate period; the pseudo-wet-bulb temperature, indicated by points B, C, and D, is about 30°C; point E represents the time at which the bobbin is essentially dry. Thermocouple depths in inches are indicated in the lower right corner. From Nissan and Kaye, reprinted by permission from *Nature* 180: 142–143, copyright 1957, Macmillan Magazines Ltd.

T/P_{sat}, but inversely with $(1 - H)$. Here, d is layer thickness, P_{sat} is the saturation vapor pressure at T, and H is the humidity fraction. Interestingly, approximations to these relationships were observed for layers of sawdust (Nelson, 1969) and jack pine litter (Van Wagner, 1979) that were losing water only through their upper surfaces. These results were further verified in unpublished studies by the writer with measured temperature distributions similar to those in Figure 15 and with predicted drying rates and plateau temperatures close to measured values for sawdust layers drying in air at temperatures from 14 to 32°C and humidity fractions from 0.25 to 0.79.

b. Data Analysis

The drying of solids under fixed external conditions (constant M_e) typically is divided into a constant-rate and two falling-rate periods (Van Wagner, 1979). In the constant-rate period, drying depends on external factors but is independent of the nature of the solid. This period is seldom seen in forest fuels except for short periods of time—when the exposed surface is covered with a water

film. The decrease in M with time t is linear. When this free water has disappeared, or the rate of water supply from the fuel interior becomes smaller than the surface evaporation rate, the first falling-rate period is triggered as the surface begins to dry. Moisture loss depends on both internal and external factors; in most fuels, the decrease in $M - M_e$ with time approximates an exponential decay. A second falling-rate period often occurs when all free water has disappeared and the fuel temperature begins to rise. This second period, while differing in mechanism from the first, also may exhibit an exponential decay, but one that usually is preceded by a time of transition from the first exponential period to the second. This type of response was observed by Anderson (1990a) in experiments on drying and wetting of forest foliage below M_{fsp} and is shown in the semilogarithmic plot of Figure 16. Similar results were reported by Nelson (1969), Anderson *et al.* (1978), and Van Wagner (1979). The fraction of evaporable moisture remaining in the fuel at any time, denoted by E, is given by

$$E = (M - M_e)/(M_{in} - M_e) \tag{35}$$

where M is the fuel particle (or layer) average moisture fraction and M_{in} is the initial value. Note that E in Eq. (35) corresponds to $(1 - E)$ in the graph of Anderson (1990a) in Figure 16.

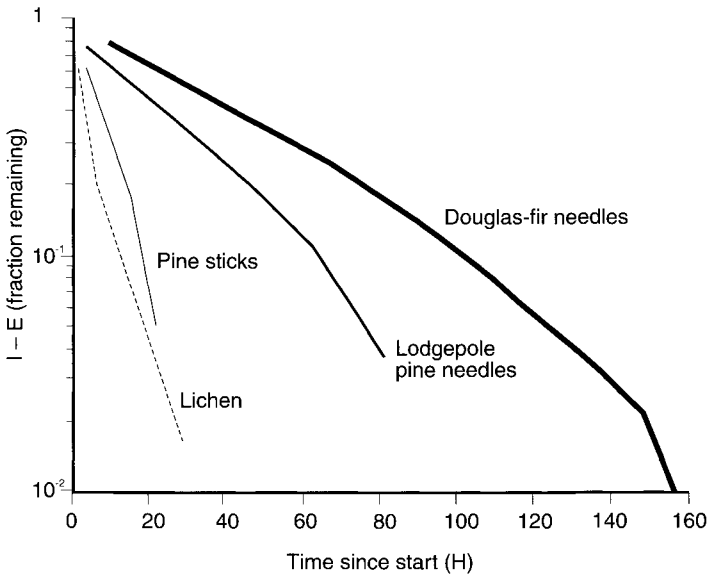

FIGURE 16 Variation in the fractional amount of evaporable moisture remaining as a function of drying time for several forest fuels. The quantity $(1 - E)$ in this figure corresponds to E in Eq. (35). The four fuels exhibit two or more drying stages. Pine sticks dry quickly when compared with pine and fir needle layers. From Anderson (1990a).

Laboratory drying (or wetting) results such as those in Figure 16 may be analyzed by means of classical diffusion theory (Crank, 1975). The theory assumes that the fuel is homogeneous and isotropic, drying is isothermal, and diffusivity D is constant. The equation for diffusion of moisture in a plane slab of thickness $2d$ (moisture exchange from both surfaces) is

$$\partial m/\partial t = D(\partial^2 m/\partial x^2) \tag{36}$$

and may be solved subject to the convective boundary condition

$$-D(\partial m/\partial x)_s = h_m(m_e - m_s) \tag{37}$$

where subscript s indicates a surface value, h_m (m s^{-1}) is the surface emission (or convective mass transfer) coefficient, and $m_e = M_e$, a constant. Though Eq. (36) strictly applies to movement below fiber saturation, the equation often is applied when free water is present for convenience. Such an analysis may fortuitously describe the moisture change in cases when the interior free water is highly mobile but drying is controlled by diffusion in the drier layers. Solving Eq. (36) subject to Eq. (37) leads to an infinite series solution that may be integrated from $x = -d$ to $x = d$ and divided by $2d$ to obtain E in the form

$$E = 2\mathrm{Bi}^2 \sum_{n=1}^{\infty} \{\exp(-\beta_n^2 \mathrm{Fo})/[\beta_n^2(\beta_n^2 + \mathrm{Bi}^2 + \mathrm{Bi})]\} \tag{38}$$

where $\mathrm{Bi} = h_m d/D$ is the mass transfer Biot number, $\mathrm{Fo} = Dt/d^2$ is the mass transfer Fourier number, and β_n is the nth positive root of the equation $\beta \tan \beta = \mathrm{Bi}$. When Fo exceeds 0.1, the series converges rapidly and an approximate solution is found by retaining only the first term for $n = 1$. If the ratio of surface resistance to internal flow resistance is small, Bi effectively approaches infinity and β_1 approaches $\pi/2$. The moisture change is driven by a significant gradient in m. Thus E is written as

$$E = (8/\pi^2) \exp(-\pi^2 Dt/4d^2) = K \exp(-t/\tau) \tag{39}$$

where constant K is sometimes assumed equal to unity and the response time is

$$\tau = 4d^2/\pi^2 D \tag{40}$$

On the other hand, when the surface resistance is relatively large and the gradient in m is small, Bi approaches zero and β_n^2 approaches Bi. In this case, E corresponding to $n = 1$ becomes

$$E = \exp(-\mathrm{BiFo}) = \exp(h_m t/d) = \exp(-t/\tau) \tag{41}$$

and τ is given by

$$\tau = d/h_m \tag{42}$$

Equations (40) and (42) display the τ-versus-d dependence described in Section II.C.3. Similar analyses are possible for other fuel shapes—the cylinder,

sphere, or square rod—and form the basis of the response time theory initially proposed by Byram (1963, unpublished). This analysis provides a convenient framework with which to interpret experimental data, but D is not a constant in fibrous materials and should be considered an integral diffusivity over the range of moisture content change. Procedures for calculating the bound water and water vapor diffusivities separately in terms of m and T (or T_f) and then combining them into an overall diffusivity are described by Nelson (2000).

The method used to evaluate integral diffusivity D_{av} from experimental data depends to some extent on the type and amount of data available. Crank (1975) shows that a semiinfinite solid dries or wets in proportion to the square root of time t and that plots of E versus $t^{1/2}$ according to Eq. (38) for constant Bi are effectively linear during roughly the first half of the exchange process. Thus when data are plentiful for short times, D_{av} for the slab may be found from a different solution of Eq. (36) written as

$$D_{av} = \pi d^2 E^2/4t = \pi d^2 s^2/4 \tag{43}$$

where s is the slope of the linear portion of a plot of E versus $t^{1/2}$ (Crank, 1975). This equation is based on three assumptions: (1) the slab dries or wets as a semiinfinite solid early in the process of moisture change, (2) shrinkage/swelling is negligible, (3) the surfaces instantaneously attain the equilibrium value, M_e. McNamara and Hart (1971) suggest using Eq. (43) in the range $0.5 \leq E \leq 1$. When data are available for more widely spaced time intervals or when $E < 0.5$, Eq. (39) may be used to obtain an estimate of D_{av} by solving for D.

For a single experiment, the effect of surface transfer on the moisture exchange process cannot be separated from that due to internal diffusion because the mass transfer correlations applicable to saturated wood surfaces are not valid for unsaturated surfaces (Plumb *et al.*, 1985; Siau and Avramidis, 1996). The effects can be separated, however, with a procedure that requires two or more experimental runs with samples of differing thickness (Choong and Skaar, 1972). A summary of the results of various investigators utilizing this procedure reports a 100-fold variation in mass transfer coefficient h_m (Siau and Avramidis, 1996). A theory for predicting h_m in the hygroscopic range was reported by Morén *et al.* (1992), and an identical relation was developed by Siau and Avramidis (1996).

3. Field Studies

Linton (1962) used the theory of diffusion in solids to describe moisture change in fuel particles in terms of a constant diffusivity and evaluated this quantity with laboratory experiments. Byram (1963, unpublished) also applied theory to the problem, but his timelag concept is applicable only to step changes between fixed initial and final values of average moisture fraction M. The oscillating

moisture content data obtained under field conditions differ from laboratory data which tend to decrease exponentially. Linton (1962) and Viney and Hatton (1989) discussed a different timelag that is useful in field studies. Their timelag is concerned with the lapse in time between the continuously varying equilibrium moisture content, M_e (defined as the M value determined by assuming equilibrium with the diurnally changing fuel temperature and relative humidity), and the actual M value for the fuel. Thus Viney and Hatton (1989) and Viney and Catchpole (1991) recommended that "timelag" be used only to denote the lag of M behind M_e and that "response time" be applied to the time needed for 63% of the total change between fixed moisture contents. Recognizing this distinction, Anderson (1990a) used "response time" to characterize the moisture exchange rates of fuels in his laboratory tests. The terminology of Viney and Catchpole is adopted in this chapter and is recommended for all future studies of fuel moisture relationships to minimize confusion.

a. Weather Factors

In addition to continuous variation in air temperature and relative humidity, other variables influencing moisture change in forest fuels include wind speed and direction, solar and longwave radiation, precipitation, canopy interception of rainfall and sunshine, filtration through fuel layers, deposition of dew, contact with fog, and source/sink effects of underlying soil. The models of Byram and Jemison (1943) describing fuel temperature and relative humidity fraction in terms of ambient values, solar radiation, and wind speed were briefly summarized in Section III.D.1. Using the iterative Newton method, Viney (1992a) presented coupled theoretical models for soil surface temperature and humidity fraction based on a surface energy balance and complex expressions for resistance to vapor transport. Viney compared predictions of T_f and H_f based on his surface balance models and on the Byram-Jemison models with values measured at the under surfaces of *Eucalyptus globulus* leaves and found that his models provided more accurate predictions of T_f and H_f than the simpler models. The mean absolute error in T_f predicted by Viney (1992a) was 0.52 K; the error for predicted H_f was 0.051.

Byram and Jemison (1943) pointed out the influence of wind on drying rate and final M_e values for forest fuels below M_{fsp}. Their data suggested that the cooling action of wind on the drying rate of irradiated fuels is greater than the tendency of wind to increase the evaporation rate. The data showed that desorption rates are slowed and M_e is increased, whereas both adsorption rates and M_e values are increased by the action of wind. Other data showed that the wind effect is reversed in the absence of radiation—i.e., drying rates for nonventilated fuels are slower than for ventilated fuels. Van Wagner (1979) conducted laboratory tests on the drying of jack pine litter at 27°C and 30% relative humidity

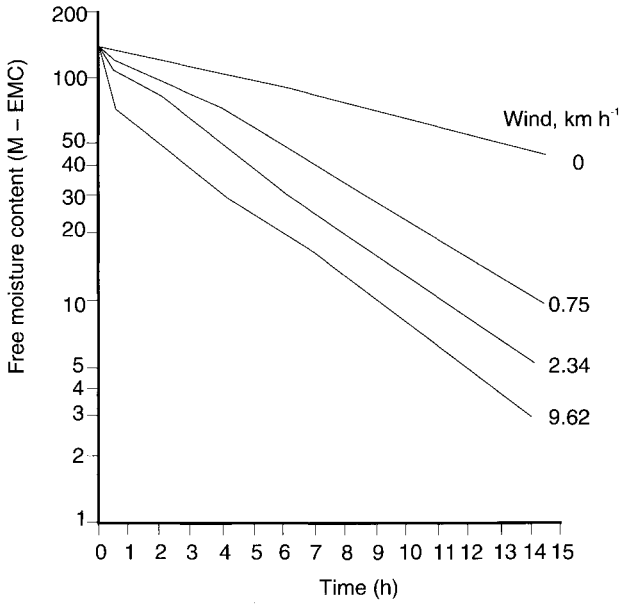

FIGURE 17 Change of free moisture content (that above the equilibrium moisture content, EMC) of jack pine litter with time at four wind speeds ranging from 0 to 9.62 km hr^{-1} (2.7 m s^{-1}). Even at the high moisture contents implied here, the effect of wind is evident only during the first hour of drying. From Van Wagner (1979).

in wind but without solar radiation; the results in Figure 17 show that the litter (which initially contained considerable free water) dried in two stages when the wind speed exceeded about 0.75 km hr^{-1} (0.2 m s^{-1}). These results indicate that differences in drying rate are established during the first hour of drying; though this first hour constitutes only a small fraction of the total drying time, a significant fraction of the moisture content change takes place during this period. For times exceeding one hour, the drying rate is roughly independent of wind speed.

The rise in average moisture content fraction, ΔM, due to rainfall has been studied by Stocks (1970) for duff (see Section II.C.2) and by Fosberg (1972) for wood cylinders. In his theoretical approach, Fosberg used numerical and analytical solutions of the diffusion equation to argue that water uptake by wood cylinders is limited by the rate at which the wood can adsorb water and that this limiting rate is of the order of 1 mm day^{-1}. He also stated that the theory predicts realistic rates of adsorption and desorption associated with precipitation and postprecipitation drying and that M increases exponentially with increasing duration of rainfall. In the empirical approach of Van Wagner (1987), ΔM

is expressed in terms of the initial value of M and the net rainfall (observed rainfall amount in the open less a correction of 0.5 mm for canopy interception). These and other treatments of ΔM due to rainfall have been critiqued by Viney (1991). Different aspects of rainfall are concerned with interception by the canopy (if present as understory or overstory) and infiltration through the litter and underlying soil but are not discussed here. These topics are treated by Helvey (1967) and Hillel (1980b).

Nocturnal condensation of water on plant surfaces can be caused by deposition of water from the atmosphere or by *distillation,* the upward transport of water vapor from the soil by turbulent diffusion (Monteith, 1963b). In a study of the effect of condensation on leaf litter moisture content, Viney and Hatton (1990) measured M for single *Eucalyptus globulus* leaves in contact with the ground at two sites in southeastern Australia. They developed a theory of condensation into which measured fluxes of net all-wave radiation, soil heat, and sensible and latent heat at the leaf surfaces were introduced to obtain a predicted ΔM (the change in average moisture fraction attributable to condensation). Good agreement between observed and predicted values is evident in Figure 18, but M is underpredicted by the model when fog is present. Viney and Hatton (1990) state that the model tends to predict a zero ΔM during fog episodes when, in fact, the leaves may have taken on moisture through direct con-

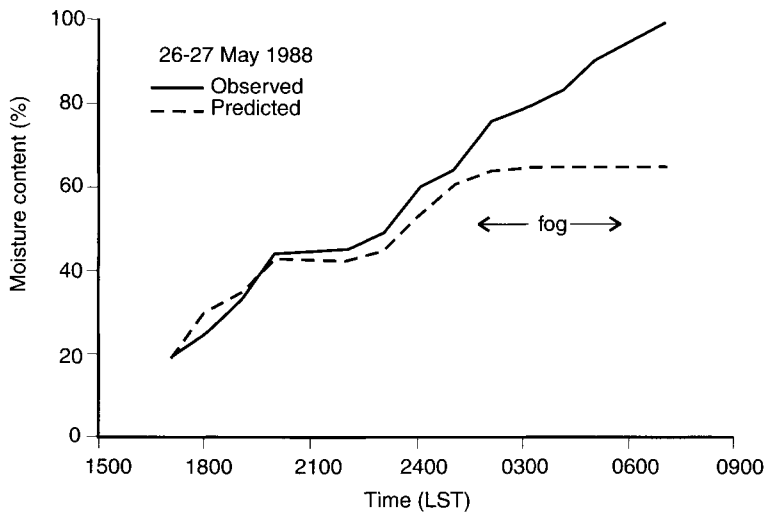

FIGURE 18 Comparison of predicted moisture contents of *Eucalyptus* leaves with those observed overnight on 26 May 1988 during experiments in eastern Australia. Moisture content change due to condensation of water vapor from the atmosphere and soil is predicted well, but the effects of fog apparently are not explained by the model. Reprinted from Agricultural and Forest Meteorology, Volume 51, Viney, N. R., and Hatton, T. J., Modelling the effect of condensation on the moisture content of forest litter, pages 51–62. Copyright 1990, with permission from Elsevier Science.

tact with fog droplets. The measured values of M during condensation also may be sensitive to fuel shape and orientation which could cause reductions in absorbed and surface-held water due to runoff (Viney, 1991).

Though the effects of soil moisture have been neglected in many studies of dead fuel moisture, at least two studies have presented evidence that the former affects the latter. Hatton *et al.* (1988) used a randomized block design to study the response of leaves of several species of *Eucalyptus* to wetted (20% dry soil weight or less) and untreated dry (8% dry weight or less) soil over a period of 48 hours. Within each cleared 8 × 8 m plot, leaves were arranged in a 2 × 1 × 0.16 m mound and also were uniformly scattered over the ground for full exposure to the weather. The leaves were held in place by nylon netting. Hatton *et al.* concluded that soil moisture influenced fuel moisture because the scattered leaves approached moisture contents of 100%, well beyond values attainable by vapor transport alone (dew was observed). In addition, leaves on top of the mound on wetted soil were about twice as moist as corresponding leaves on the dry soil. This difference was explained in terms of more water available for distillation from the wetter soil. In a different study conducted in aspen stands of central Alberta, Rothwell *et al.* (1991) measured the water potential and volumetric water content (in %) at locations 2–3 cm above and below the transition zone between the litter layer and mineral soil. The authors concluded, on the basis that water flows from higher to lower levels of water potential, that soil water affects fuel availability and fire behavior in stands of aspen because upward capillary flow from the soil kept the litter moist in their experiments.

b. Prediction Models

Viney and Hatton (1989) measured the moisture content of dead leaves, bark, and twigs of *Eucalyptus macrorhyncha* and *Eucalyptus rossii* in contact with the ground for the purpose of assessing models for predicting the moisture content of fine fuels. They reported significant differences in equilibrium moisture fraction M_e within the three fuel types of the study and stated that submodels for dew and distillation should be included in models to be used in open or lightly foliated areas. Viney and Catchpole (1991) and Viney (1992a, 1992b) developed a method for estimating fuel moisture response time and timelag (the lag of fuel moisture fraction M behind M_e) from field observations. The basis of their method is shown in Figure 19 in which it is assumed that both M and M_e follow a 24-hour sinusoidal cycle. In present notation, the equations describing such data are

$$M(t) = M_{av} + a\,\mathrm{Sin}[\omega(t - \varphi_m)] \tag{44}$$

$$M_e(t) = E_{av} + A\,\mathrm{Sin}[\omega(t - \varphi_e)] \tag{45}$$

where M_{av}, E_{av}, a, and A are constants obtained from least squares regression analysis, t is time (h), φ_m and φ_e (h) are phase lags relative to midnight, and ω

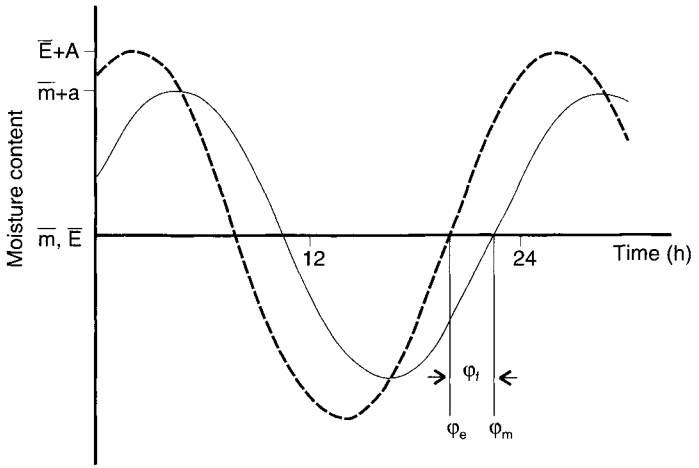

FIGURE 19 Idealized sinusoidal variation in equilibrium (dashed curve) and fuel (solid curve) moisture contents with time under field conditions. The average values of E and M shown in this figure are represented as E_{av} and M_{av}, respectively, in Eqs. (44) and (45). The timelag φ_f is the difference in phase for the two curves. From Viney (1992a, 1992b).

is the angular frequency given by $\omega = \pi/12$ hr^{-1}. Hourly observations of M and M_e over a period of several days are filtered with a time series decomposition algorithm to eliminate long-term trends and random fluctuations and to obtain φ_m and φ_e from the two sets of data. As Figure 19 shows, the difference $\varphi_m - \varphi_e$ is the timelag (or phase lag) of the fuel, φ_f. The final step is to determine response time τ from

$$\tau = (1/\omega)\,\mathrm{Tan}(\omega\varphi_f) \tag{46}$$

The derivation of Eq. (46) is based on three additional assumptions: (1) the resistance to internal moisture transport is small compared to that at the fuel surface, (2) τ is constant during the diurnal cycle, and (3) time since midnight of the day prior to the first day of the measurement period ($t = 0$) is large compared with the fuel's response time. These assumptions are reasonable for fine or poorly ventilated fuels in which moisture is exchanged with little or no gradient in moisture content. An alternative to evaluating φ_f with the sinusoidal assumptions is to represent the two data sets with cubic spline interpolations and then choose the value of φ_f that maximizes correlation between the two sets. In a further modification of these methods, Catchpole *et al.* (in press) combined spline interpolation with the sorption isotherm in Eq. (26) to find estimates of M_e and τ without assuming sinusoidal variation in M and M_e. According to Catchpole *et al.*, tests of the model with data collected in Tasmanian buttongrass moorland and Western Australian mallee shrubland have given

them "some confidence in the robustness of the method and the appropriateness of the model." The methods described here should be used only for fuels with short (3 h or less) response times and would apply during periods of sorption-controlled moisture exchange rather than periods of rainfall or evaporation and condensation.

In larger fuels or fuels that dry in the presence of moisture content gradients, internal resistance exceeds that at the surface. Viney (1992a, 1992b) pointed out that such conditions require solution of the diffusion equation appropriate for the type of fuel particle under consideration. To evaluate the constant moisture diffusivity, D, for different particles, he solved the diffusion equations applicable to the semiinfinite solid (representing a layer of leaf or needle litter in contact with the ground), the slab (a flat leaf), the cylinder (a twig or needle), and the long square rod (a fuel moisture indicator stick)—all subject to sinusoidal surface boundary conditions. A parameter common to all four solutions is the dimensionless number, kd, where k is given by

$$k = (\omega/2D)^{1/2} \tag{47}$$

and d is the depth of interest for the semiinfinite solid, thickness of the slab, diameter of the cylinder, or side length of the square rod. Though solutions for the average moisture fraction were derived analytically, their complexity precluded evaluation of kd, and hence D. Numerical representations of φ_f for the four fuel arrangements are shown in Figure 20. If the timelag is evaluated from

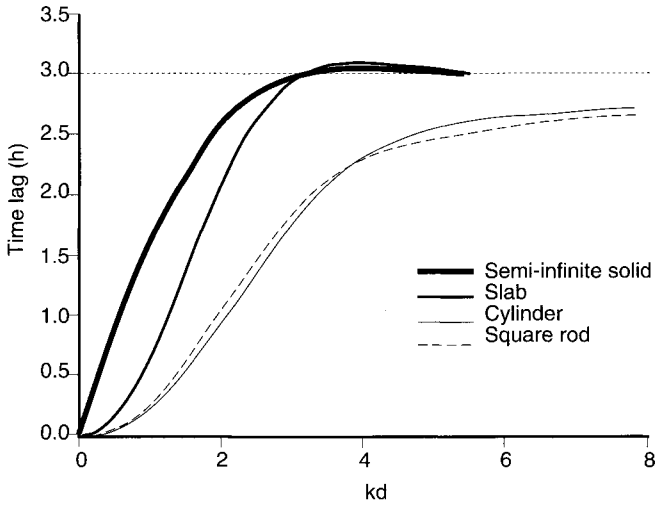

FIGURE 20 Relationship between the fuel timelag and dimensionless parameter kd for the four fuel shapes indicated. Quantity d represents the depth for which the timelag is desired in a semiinfinite solid, thickness for a slab, diameter for a cylinder, and side length for a square rod. From Viney (1992a, 1992b).

field data and d is known, then k may be determined from Figure 20 and used in Eq. (47) to compute D. Viney (1992a, 1992b) compared his calculated D values for leaf and twig data from the Viney and Hatton (1989) study with those reported by Linton (1962) and found good agreement for leaves and 6 mm twigs; his D for 3 mm twigs slightly exceeded Linton's values. In a different comparison, Viney's D for a lodgepole pine litter layer was within the range of corresponding values measured by Anderson (1990a).

Several investigators have developed diurnal prediction models from field data. Fosberg (1975) derived a model for conifer litter and duff from mass conservation equations for water vapor and the first law of thermodynamics. The physical properties of litter and duff horizons were taken from measurements on ponderosa pine and lodgepole pine layers or from the literature. Fosberg adapted his model to field conditions by introducing time-dependent boundary conditions consisting of step changes of arbitrary duration and magnitude. Though he did not compare his computed M-versus-t curves with data from laboratory or field experiments, Fosberg's predicted response times based on layer properties were close to several values in the literature. A predictive model of moisture content and evaporative loss in the litter of a mixed deciduous forest was reported by Moore and Swank (1975). Weather data requirements included daily totals for sunlight and rainfall and daytime means for atmospheric temperature and relative humidity. The model contains three hydrologic compartments—atmosphere, litter, and soil. In addition to evaporation from litter to the atmosphere and liquid drainage from litter to the soil, litterfall and litter dry weight (or decomposition) are modeled. Though they are acknowledged as important at times, atmospheric condensation and upward flow of moisture from the soil are not modeled. Independent data for validating model predictions during a 7-day period in the summer and an 11-day period during the winter were collected at the Coweeta Hydrologic Laboratory in western North Carolina. Predicted moisture contents usually were within the error limits of the experimental values. Simulated evaporation agreed to within 13% of the measured evaporation but was more accurate for the first two days after rain than under drier conditions. Moisture content comparisons during an additional 80-day verification study gave similar results. A model for computing fine fuel moisture content during the diurnal cycle was developed by Van Wagner (1987) using jack pine and lodgepole pine data; it is based on the assumption that wetting and drying by vapor exchange with the atmosphere are exponential, whereas wetting due to rainfall depends on rainfall amount and yesterday's fine fuel moisture content. In a different study, Nelson (2000) used diurnal weather and moisture content data from two field sites in the eastern United States to guide the formulation of a numerical model for computing hourly changes in the moisture content and temperature of 1.27-cm-diameter ponderosa pine dowels. In the model, water moves by capillarity and combined bound

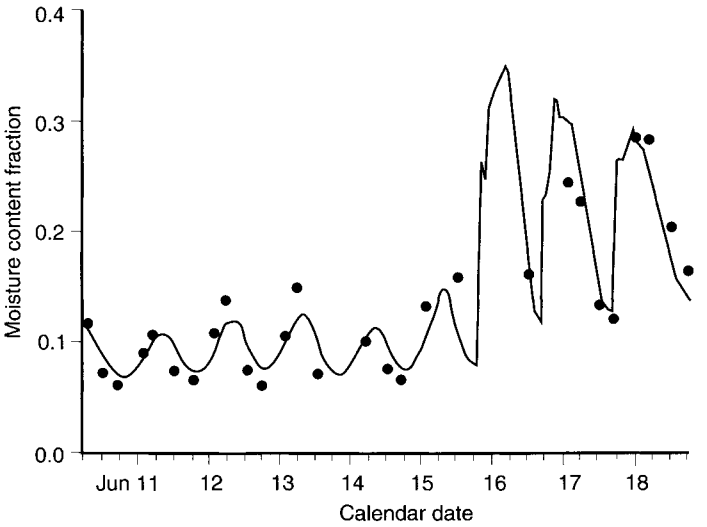

FIGURE 21 Comparison between predicted and observed moisture contents for 10-h fuel indicator sticks under field conditions in western Montana during June 1996. Rainfall occurred prior to midnight on June 15 and 16 and at about 1800 on June 17. Solid lines represent predictions; circles denote observations. From Nelson (2000).

water/water vapor diffusion. Either precipitation, evaporation, condensation, or sorption determines the surface boundary condition; water takeup due to fog is not considered. The model accepts data from remote automatic weather stations (RAWS). Input consists of hourly readings of air temperature and relative humidity, solar radiation flux, and rainfall amount; changes in the four variables from one reading to the next are assumed to be linear. Independent observations for testing the model were compared with predicted values; predictions generally agreed with observations to within the accuracy of the experimental moisture content data, but rates of response appear to be slightly slower than the observed rates (Figure 21).

IV. MOISTURE CONTENT ESTIMATION

Aside from prediction models, other means of estimating the moisture content of live and dead fuels include weighing, correlation with Advanced Very High Resolution Radiometer (AVHRR) data from NOAA satellites, resistance meters, and artificial fuel sticks available with RAWS. Moisture content calculations require a sample ovendry weight. Drying in the usual convection oven is slow, and the fuel is subject to loss of volatiles if dried too long at a high temperature.

In the literature, drying temperatures for wood and foliage range from 60 to 105°C. Perhaps the safest procedure for foliage is to dry at 100°C until a constant weight is reached. This method, of course, requires frequent weighings to prevent loss of volatiles due to prolonged drying. King and Linton (1963) concluded that materials ovendried prior to testing adsorb water about half as fast as those that have been dried only to a low moisture content. Thus experimental error may be reduced by determining ovendry weights after the measurements are made. To avoid the slowness and labor intensiveness of this method, instruments composed of a small balance and oven (or electric heater) have been developed, but this method is suitable only for small samples. Commercially available kitchen microwave ovens were tested by Norum and Fischer (1980). Wet duff (up to 230% moisture content) and 0 to 0.64-cm-diameter branchwood (up to 90%) samples weighing about 40 g were ovendried in 24 minutes or less. Live fuel moisture content can be estimated from satellites with the Normalized Difference Vegetation Index (NDVI) which operates by sensing red and near infrared radiation reflected from the surfaces of green or curing vegetation. Burgan *et al.* (1991) showed that the NDVI is useful for calculating overall site moisture content, whereas Piñol *et al.* (1998) developed a rapid method for measuring the moisture content of individual plants. Chladil and Nunez (1995) used AVHRR to follow curing of grasslands in Tasmania and concluded that the NDVI gives good results for fuel and soil moisture contents but is not a suitable standalone system for fire managers. Electrical resistance meters are useful for estimating the moisture content of wood in the hygroscopic range but are sensitive to contact resistance and presence of a moisture gradient (Skaar, 1988). Other factors mentioned by Clark and Roberts (1982) include wood species, density, and grain angle; they used a minimum of 20 samples for calibrating their meter to the species utilized in their study. The moisture content of the 10-h fuel moisture indicator sticks used in the U.S. National Fire Danger Rating System (Bradshaw *et al.*, 1983) may be estimated with an artificial fuel moisture and fuel temperature stick that can be supplied with RAWS installations. The stick is equipped with sensors to measure its relative humidity and temperature, from which a moisture content is derived.

Most fire suppression and control organizations maintain a system with which they assess the moisture content of the live and dead fuels within their areas of jurisdiction. For operational applications, equations for estimating fuel moisture content are found in fire danger rating and fire behavior prediction systems around the world. A brief description of how moisture content is evaluated in several of the fire danger rating systems is presented in Chapter 9 in this book. In addition, operational models for prediction of dead fuel moisture content in the hygroscopic range have been discussed and compared by Viney (1991, 1992a). The reader is referred to Van Wagner (1987) and to the Forestry Canada Fire Danger Group (1992) for details of the Canadian systems, to Bradshaw *et al.* (1983) and Rothermel *et al.* (1986) for the American systems, and

to Noble *et al.* (1980) and Sneeuwjagt and Peet (1985) for the Australian systems. Another aspect of fire danger involves water loss from deep soils and large fuels during extended dry periods. As before, the reader is referred to pertinent papers on the subject. Discussions of drought and drought indexes are given in key papers by Van Wagner (1987), Keetch and Byram (1968) and Alexander (1992), and Mount (1972) for the Canadian, American, and Australian systems, respectively.

NOTATION

Roman Letters

C	specific water capacity	m^{-1}, $s^2\ m^{-2}$
c	constant-pressure specific heat	$J\ kg^{-1}\ K^{-1}$
D	local moisture diffusivity	$m^2\ s^{-1}$
D_{av}	particle or layer average moisture diffusivity	$m^2\ s^{-1}$
D_h	hydraulic diffusivity	$m^2\ s^{-1}$
d	particle radius or half-thickness, layer depth	m
E	fraction of evaporable moisture	
e	base of Naperian logarithms	
G	Gibbs free energy	$J\ mol^{-1}$
g	gravitational acceleration	$9.8\ m\ s^{-2}$
H	ambient air relative humidity fraction	
h	hydrostatic pressure head	m
h_m	surface emission coefficient	$m\ s^{-1}$
J	mass flux	$kg\ m^{-2}\ s^{-1}$
K	specific permeability	m^2
k	parameter in Eq. (47), thermal conductivity	m^{-1}, $J\ m^{-1}\ s^{-1}\ K^{-1}$
L	root length	m
ln	Naperian logarithm	
M	particle or layer average moisture content fraction	
M_w	molecular weight of water	$0.018\ kg\ mol^{-1}$
M_1	M value when $\psi = -1\ J\ kg^{-1}$	
m	local moisture content fraction	
P	fluid pressure, saturation vapor pressure	$J\ m^{-3}$

P_b	bound water spreading pressure	J m^{-2}
P_c	capillary pressure	J m^{-3}
p	gas phase partial pressure	J m^{-3}
$\mathcal{Q}$	transpiration or evapotranspiration rate	m s^{-1}
$\mathcal{Q}_f$	demand to heat dry fuel from ambient to 400°C	kJ kg^{-1}
$\mathcal{Q}_M$	heat required to evaporate water at 100°C	kJ kg^{-1}
$\mathcal{Q}_T$	heat of ignition	kJ kg^{-1}
q	heat flux	J m^{-2} s^{-1}
RWC	relative water content	
r	radial distance, flow resistance, mean radius of the gas–liquid interface	m; s m^{-1}, bar-s m^{-1}, m^3 kg^{-1} s^{-1}; m
r_1, r_2	radii of curvature of a gas–liquid interface	m
S	liquid water saturation	
s	slope of E versus $t^{1/2}$ plot	$s^{-1/2}$
T	ambient air temperature	K
t	time	s, hr
U	root sink strength	kg m^{-3} s^{-1}
V	specific volume	m^3 kg^{-1}
v	velocity	m s^{-1}
W	plant tissue weight, duff weight consumed by fire	kg, kg m^{-2}
w	rate of evaporation	kg m^{-3} s^{-1}
x	coordinate in direction of moisture transport	m
z	vertical distance from reference elevation	m

Greek Letters

α	hysteresis ratio	
β	fuel layer packing ratio	
β_n	nth root of $\beta\mathrm{Tan}\beta = \mathrm{Bi}$	
γ	surface tension of water	J m^{-2}
Δ	finite change in associated variable	
δ	fuel layer depth	m

ε	fractional void volume	
η	kinematic viscosity	$m^2\ s^{-1}$
Θ	temperature	°C
θ	volumetric soil water content	
κ	hydraulic conductivity	$m\ s^{-1}$, kg-s m^{-1}
λ	latent heat of evaporation/condensation at T	$J\ kg^{-1}$
λ_d	differential heat of sorption	$J\ kg^{-1}$
μ	chemical potential	$J\ mol^{-1}$
ρ	mass density	$kg\ m^{-3}$
ρ_r	root density	m^{-2}
σ	particle surface-to-volume ratio	m^{-1}
τ	moisture response time	s, hr
φ	sinusoidal phase lag	hr
ϕ	phase volume fraction	
ψ	water potential	$J\ m^{-3}$, $J\ kg^{-1}$
ω	angular frequency	$\pi/12\ hr^{-1}$

Dimensionless Groups

Bi	mass transfer Biot number
Fo	mass transfer Fourier number

Constants

R	universal gas constant	$8.32\ J\ mol^{-1}\ K^{-1}$

Subscripts

a	atmospheric air, dry air component of the gas phase
av	particle or layer average
b	bound water phase
c	current state
cw	cell wall
d	dry state

e	equilibrium state
f	fuel
fsp	fiber saturation point
g	gravitational potential, gas phase
h	hydraulic head
i	phase designator
in	initial state
l	leaf
m	matric potential, moisture
m(a)	apoplast matric potential
max	maximum value
o	reference state
p	pressure potential
pwb	pseudo-wet-bulb value
r	root
s	solution (or osmotic) potential, solid phase, surface
s(a)	apoplast solution (or osmotic) potential
so	soil
sat	saturated state
T	total value
t	turgid state
v	water vapor component of the gas phase
va	vacuole, vapor in ambient air
w	liquid water phase

ADDITIONAL READING

Brown, R. W. (1995). The water relations of range plants: adaptations to water deficits. *In* "Wildland Plants: Physiological Ecology and Developmental Morphology" (D. J. Bedunah and R. E. Sosebee, Eds.), pp. 291–413. Society for Range Management, Denver.

Marshall, M. J., Holmes, J. W., and Rose, C. W. (1996). "Soil Physics," 3rd ed. Cambridge University Press, Cambridge.

Smith, J. A. C., and Griffiths, H. (1993). "Water Deficits: Plant Responses from Cell to Community." BIOS Scientific Publishers, Oxford.

Waring, R. H., and Running, S. W. (1998). "Forest Ecosystems: Analysis at Multiple Scales," 2nd ed., Chapter 2. Academic Press, San Diego.

REFERENCES

Albini, F. A. (1980). "Thermochemical Properties of Flame Gases from Fine Wildland Fuels." Research Paper INT-243. USDA Forest Service, Intermountain Forest and Range Experiment Station, Ogden.

Albini, F. A., and Reinhardt, E. D. (1995). Modeling ignition and burning rate of large woody natural fuels. *Int. J. Wildland Fire* **5**, 81–91.

Alessi, S., Prunty, L., and Schuh, W. M. (1992). Infiltration simulations among five hydraulic property models. *Soil Sci. Soc. Am. J.* **56**, 675–682.

Alexander, M. E. (1992). The Keetch-Byram drought index: A corrigendum. *Bull. Am. Meteorol. Soc.* **73**, 61.

Alexander, M. E., Stocks, B. J., Wotton, B. M., and Lanoville, R. A. (1998). An example of multifaceted wildland fire research: The International Crown Fire Modelling Experiment. *In* "Proceedings, III International Conference on Forest Fire Research/14th Conference on Fire and Forest Meteorology," pp. 83–112. University of Coimbra.

Anderson, H. E. (1990a). Moisture diffusivity and response time in fine forest fuels. *Can. J. For. Res.* **20**, 315–325.

Anderson, H. E. (1990b). "Predicting Equilibrium Moisture Content of Some Foliar Forest Litter in the Northern Rocky Mountains." Research Paper INT-429. USDA Forest Service, Intermountain Research Station, Ogden.

Anderson, H. E., Schuette, R. D., and Mutch, R. W. (1978). "Timelag and Equilibrium Moisture Content of Ponderosa Pine Needles." Research Paper INT-202. USDA Forest Service, Intermountain Forest and Range Experiment Station, Ogden.

Anderson, N. T., and McCarthy, J. L. (1963). Two-parameter isotherm equation for fiber-water systems. *Ind. Eng. Chem. Process Des. Develop.* **2**, 103–105.

Babbitt, J. D. (1950). On the differential equations of diffusion. *Can. J. Res.* **A-28**, 449–474.

Barkas, W.W. (1949). "The Swelling of Wood Under Stress." Department of Scientific and Industrial Research, Forest Products Research, HSMO, London.

Blackmarr, W. H. (1971). "Equilibrium Moisture Content of Common Fine Fuels Found in Southeastern Forests." Research Paper SE-74. USDA Forest Service, Southeastern Forest Experiment Station, Asheville.

Blackmarr, W. H. (1972). "Moisture Content Influences Ignitability of Slash Pine Litter." Research Paper SE-173. USDA Forest Service, Southeastern Forest Experiment Station, Asheville.

Blackmarr, W. H., and Flanner, W. B. (1968). "Seasonal and Diurnal Variation in Moisture Content of Six Species of Pocosin Shrubs." Research Paper SE-33. USDA Forest Service, Southeastern Forest Experiment Station, Asheville.

Blackmarr, W. H., and Flanner, W. B. (1975). "Moisture Variation in Selected Pocosin Shrubs of Eastern North Carolina." Research Paper SE-124. USDA Forest Service, Southeastern Forest Experiment Station, Asheville.

Bradshaw, L. S., Deeming, J. D., Burgan, R. E., and Cohen, J. D. (1983). "The 1978 National Fire-Danger Rating System: Technical Documentation." General Technical Report INT-169. USDA Forest Service, Intermountain Forest and Range Experiment Station, Ogden.

Brown, H. P., Panshin, A. J., and Forsaith, C. C. (1949). "Textbook of Wood Technology, Vol. 1," 1st ed. McGraw-Hill, New York.

Brown, J. K., Booth, G. D., and Simmerman, D. G. (1989). Seasonal change in live fuel moisture of understory plants in western U.S. aspen. *In* "Proceedings of the Tenth Conference on Fire and Forest Meteorology" (D. C. MacIver, H. Auld, and R. Whitewood, Eds.), pp. 406–412. Forestry Canada, Environment Canada, Ottawa.

Brown, R. W. (1977). Water relations of range plants. *In* "Rangeland Plant Physiology" (R. E. Sosebee, Ed.), Range Science Series 4, pp. 97–140. Society for Range Management, Denver.

Browning, B. L. (1963). "The Chemistry of Wood." John Wiley, New York.

Burgan, R. E., Hartford, R. A., Eidenshink, J. C., and Werth, L. F. (1991). Estimation of vegetation greenness and site moisture using AVHRR data. *In* "Proceedings of the Eleventh Conference on Fire and Forest Meteorology" (P. L. Andrews and D. F. Potts, Eds.), pp. 17–24. Society of American Foresters, Bethesda.

Byram, G. M. (1959). Combustion of forest fuels. *In* "Forest Fire: Control and Use" (K. P. Davis, Ed.), pp. 61–89. McGraw-Hill, New York.

Byram, G. M. (1963). "An Analysis of the Drying Process in Forest Fuel Material." Unpublished report. USDA Forest Service, Fire Sciences Laboratory, Rocky Mountain Research Station, Missoula.

Byram, G. M., and Jemison, G. M. (1943). Solar radiation and forest fuel moisture. *J. Agric. Res.* **67**, 149–176.

Campbell, G. S., Jungbauer, J. D., Jr., Shiozawa, S., and Hungerford, R. D. (1993). A one-parameter equation for water sorption isotherms of soils. *Soil Sci.* **156**, 302–305.

Catchpole, E. A., Catchpole, W. R., Viney, N. R., McCaw, W. L., and Marsden-Smedley, J. B. Modelling fuel response time and equilibrium moisture content from field data. Accepted for publication, *Int. J. Wildland Fire.*

Chandler, C., Cheney, P., Thomas, P., Trabaud, L., and Williams, D. (1983). "Fire in Forestry: Vol. I." John Wiley, New York.

Chladil, M. A., and Nunez, M. (1995). Assessing grassland moisture and biomass in Tasmania—The application of remote sensing and empirical models for a cloudy environment. *Int. J. Wildland Fire* **5**, 165–171.

Choong, E. T. (1965). Diffusion coefficients of softwoods by steady-state and theoretical methods. *For. Prod. J.* **15**, 21–27.

Choong, E. T., and Skaar, C. (1972). Diffusivity and surface emissivity in wood drying. *Wood Fiber* **4**, 80–86.

Choudhury, B. J., and Monteith, J. L. (1988). A four-layer model for the heat budget of homogeneous land surfaces. *Quart. J. Roy. Meteorol. Soc.* **114**, 373–398.

Christensen, G. N. (1965). The rate of sorption of water vapor by thin materials. *In* "Humidity and Moisture: Measurement and Control in Science and Industry" (A. Wexler, Ed.), Vol. 4, pp. 279–293. Reinhold, New York.

Chrosciewicz, Z. (1986). Foliar moisture content variations in four coniferous tree species of central Alberta. *Can. J. For. Res.* **16**, 157–162.

Clark, B., and Roberts, F. (1982). A belt weather kit accessory for measuring woody fuel moisture. *Fire Manage. Notes* **43**, 25–26.

Cloutier, A., and Fortin, Y. (1991). Moisture content—water potential relationship of wood from saturated to dry conditions. *Wood Sci. Tech.* **25**, 263–280.

Cloutier, A., and Fortin, Y. (1993). A model of moisture movement in wood based on water potential and the determination of the effective water conductivity. *Wood Sci. Tech.* **27**, 95–114.

Comstock, G. L. (1970). Directional permeability of softwoods. *Wood Fiber* **1**, 283–289.

Coté, W. A., Jr. (1967). "Wood Ultrastructure." University of Washington Press, Seattle.

Countryman, C. (1974). Moisture in living fuels affects fire behavior. *Fire Manage. Notes* **35**, 10–13.

Cowan, I. R. (1965). Transport of water in the soil-plant-atmosphere system. *J. Appl. Ecol.* **2**, 221–239.

Cowan, I. R., and Milthorpe, F. L. (1968). Plant factors influencing the water status of plant tissues. *In* "Water Deficits and Plant Growth" (T. T. Kozlowski, Ed.), Vol. 1, pp. 137–193. Academic Press, New York.

Crank, J. (1975). "The Mathematics of Diffusion," 2nd ed. Clarendon Press, Oxford.

Davis, K. P. (1959). "Forest Fire: Control and Use." McGraw-Hill, New York.

Dunlap, M. E. (1932). The drying rate of hardwood-forest leaves. *J. For.* **30**, 421–423.

Federer, C. A. (1979). A soil-plant-atmosphere model for transpiration and availability of soil water. *Water Resources Res.* **15**, 555–562.

Fernandez, M. L., and Howell, J. R. (1997). Convective drying model of southern pine. *Drying Tech.* **15**, 2343–2375.

Flowers, T. J., and Yeo, A. R. (1992). "Solute Transport in Plants." Blackie Academic & Professional, Chapman & Hall, Glasgow.

Fons, W. L. (1950). Heating and ignition of small wood cylinders. *Ind. Engr. Chem.* **42**, 2130–2133.

Forestry Canada Fire Danger Group. (1992). "Development and Structure of the Canadian Forest Fire Behavior Prediction System." Information Report ST-X-3. Forestry Canada, Science and Sustainable Development Directorate, Ottawa.

Fosberg, M. A. (1972). Theory of precipitation effects on dead cylindrical fuels. *For. Sci.* **18**, 98–108.

Fosberg, M. A. (1975). "Heat and Water Vapor Flux in Conifer Forest Litter and Duff: A Theoretical Model." Research Paper RM-152. USDA Forest Service, Rocky Mountain Forest and Range Experiment Station, Fort Collins.

Fosberg, M. A. (1977). "Heat and Water Vapor Transport Properties in Conifer Duff and Humus." Research Paper RM-195. USDA Forest Service, Rocky Mountain Forest and Range Experiment Station, Fort Collins.

Gardner, W. R., and Ehlig, C. F. (1965). Physical aspects of the internal water relations of plant leaves. *Plant Physiol.* **40**, 705–710.

Gary, H. L. (1971). Seasonal and diurnal changes in moisture contents and water deficits of Engelmann spruce needles. *Bot. Gaz.* **132**, 327–332.

Gong, L., and Plumb, O. A. (1994). The effect of heterogeneity on wood drying, part 1: Model development and predictions. *Drying Tech.* **12**, 1983–2001.

Hart, C. A. (1964). Principles of moisture movement in wood. *For. Prod. J.* **14**, 207–214.

Hart, C. A., and Thomas, R. J. (1967). Mechanism of bordered pit aspiration as caused by capillarity. *For. Prod. J.* **17**, 61–68.

Hatton, T. J., Viney, N. R., Catchpole, E. A., and de Mestre, N. J. (1988). The influence of soil moisture on *Eucalyptus* leaf litter moisture. *For. Sci.* **34**, 292–301.

Helvy, J. D. (1967). Interception by eastern white pine. *Water Resources Res.* **3**, 723–729.

Hillel, D. (1980a). "Fundamentals of Soil Physics." Academic Press, New York.

Hillel, D. (1980b). "Applications of Soil Physics." Academic Press, New York.

Hough, W. A. (1973). "Fuel and Weather Influence Wildfires in Sand Pine Forests." Research Paper SE-106. USDA Forest Service, Southeastern Forest Experiment Station, Asheville.

Howard, E. A., III. (1978). A simple model for estimating the moisture content of living vegetation as potential wildfire fuel. *In* "Preprint Volume, Fifth National Conference on Fire and Forest Meteorology," pp. 20–23. American Meteorological Society, Boston.

Jarvis, P. G. (1975). Water transfer in plants. *In* "Heat and Mass Transfer in the Biosphere. Part I. Transfer Processes in the Plant Environment" (D. A. de Vries and N. H. Afgan, Eds.), pp. 369–394. Scripta Book Company, Washington, DC.

Jury, W. A., Gardner, W. R., and Gardner, W. H. (1991). "Soil Physics," 5th ed. Academic Press, San Diego.

Katchalsky, A., and Curran, P. F. (1965). "Nonequilibrium Thermodynamics in Biophysics." Harvard University Press, Cambridge.

Keetch, J. J., and Byram, G. M. (1968). "A Drought Index for Forest Fire Control." Research Paper SE-38. USDA Forest Service, Southeastern Forest Experiment Station, Asheville.

Kelsey, K. E. (1957). The sorption of water vapour by wood. *Aust. J. Appl. Sci.* **8**, 42–54.

King, A. R., and Linton, M. (1963). Moisture variation in forest fuels: the rate of response to climate change. *Aust. J. Appl. Sci.* **14**, 38–49.

King, N. R. (1973). The influence of water vapour on the emission spectra of flames. *Combust. Sci. Tech.* **6**, 247–256.

Kozlowski, T. T., and Clausen, J. J. (1965). Changes in moisture contents and dry weights of buds and leaves of forest trees. *Bot. Gaz.* **126**, 20–26.

Kozlowski, T. T., and Pallardy, S. G. (1997). "Physiology of Woody Plants," 2nd ed. Academic Press, San Diego.

Kramer, P. J., and Boyer, J. S. (1995). "Water Relations of Plants and Soils." Academic Press, New York.

Kramer, P. J., and Kozlowski, T. T. (1979). "Physiology of Woody Plants." Academic Press, Orlando.

Kreith, F., and Sellers, W. D. (1975). General principles of natural evaporation. *In* "Heat and Mass Transfer in the Biosphere. Part I. Transfer Processes in the Plant Environment" (D. A. de Vries and N. H. Afgan, Eds.), pp. 207–227. Scripta Book Company, Washington, DC.

Lemon, E., Stewart, D. W., and Shawcroft, R. W. (1971). The sun's work in a cornfield. *Science* **174**, 371–378.

Linton, M. (1962). "Report on Moisture Variation in Forest Fuels—Prediction of Moisture Content." Commonwealth Scientific and Industrial Research Organization, Division of Physical Chemistry, Melbourne.

Little, C. H. A. (1970). Seasonal changes in carbohydrate and moisture content in needles of balsam fir (*Abies balsamea*). *Can. J. Bot.* **48**, 2021–2028.

Lopushinsky, W., and Klock, G. O. (1974). Transpiration of conifer seedlings in relation to soil water potential. *For. Sci.* **20**, 181–186.

Luke, R. H., and McArthur, A. G. (1978). "Bushfires in Australia." Australian Government Publishing Service, Canberra.

McGilvary, J. M., and Barnett, J. P. (1988). Increasing speed, accuracy, and safety of pressure chamber determinations of plant moisture stress. *Tree Planters' Notes* **39**, 3–4.

McNamara, W. S., and Hart, C. A. (1971). An analysis of interval and average diffusion coefficients for unsteady-state movement of moisture in wood. *Wood Sci.* **4**, 37–45.

Monteith, J. L. (1963a). Gas exchange in plant communities. *In* "Environmental Control of Plant Growth" (L. T. Evans, Ed.), pp. 95–112. Academic Press, New York.

Monteith, J. L. (1963b). Dew: Facts and fallacies. *In* "The Water Relations of Plants" (A. J. Rutter and F. H. Whitehead, Eds.), pp. 37–56. John Wiley, New York.

Monteith, J. L. (1980). The development and extension of Penman's evaporation formula. *In* "Applications of Soil Physics" (D. Hillel, Ed.), pp. 247–253. Academic Press, New York.

Monteith, J. L., Szeicz, G., and Waggoner, P. E. (1965). The measurement and control of stomatal resistance in the field. *J. Appl. Ecol.* **2**, 345–355.

Moore, A., and Swank, W. T. (1975). A model of water content and evaporation for hardwood leaf litter. *In* "Mineral Cycling in Southeastern Ecosystems," (F. G. Howell, J. B. Gentry, and M. H. Smith, Eds.), pp. 58–69. ERDA Symposium Series, Technical Information Center, Office of Public Affairs, U.S. Energy Research and Development Administration, Oak Ridge.

Morén, T., Salin, J.-G., and Söderström, O. (1992). Determination of the surface emission factors in wood sorption experiments. *In* "Understanding the Wood Drying Process: A Synthesis of Theory and Practice," (M. Vanek, Ed.), pp. 69–73. 3rd IUFRO International Wood Drying Conference, Boku, Vienna.

Mount, A. B. (1972). "The Derivation and Testing of a Soil Dryness Index Using Run-off Data." Bulletin No. 4. Tasmania Forestry Commission, Hobart.

Nelson, R. M., Jr. (1969). "Some Factors Affecting the Moisture Timelags of Woody Materials." Research Paper SE-44. USDA Forest Service, Southeastern Forest Experiment Station, Asheville.

Nelson, R. M., Jr. (1984). A method for describing equilibrium moisture content of forest fuels. *Can. J. For. Res.* **14**, 597–600.

Nelson, R. M., Jr. (1986a). Diffusion of bound water in wood. Part 1: The driving force. *Wood Sci. Tech.* **20**, 125–135.

Nelson, R. M., Jr. (1986b). Diffusion of bound water in wood. Part 2: A model for isothermal diffusion. *Wood Sci. Tech.* **20**, 235–251.

Nelson, R. M., Jr. (2000). Prediction of diurnal change in 10-hour fuel stick moisture content. *Can. J. For. Res.* **30**, 1071–1087.

Nissan, A. H., and Kaye, W. G. (1957). Mechanism of drying of thick porous bodies during the falling-rate period. *Nature* **180**, 142–143.

Nissan, A. H., Kaye, W. G., and Bell, J. R. (1959). Mechanism of drying thick porous bodies during the falling rate period. I. The pseudo-wet-bulb temperature. *AIChE J.* **5**, 103–110.

Noble, I. R., Bary, G. A. V., and Gill, A. M. (1980). McArthur's fire-danger meters expressed as equations. *Aust. J. Ecol.* **5**, 201–203.

Norum, R. A., and Fischer, W. C. (1980). "Determining the Moisture Content of Some Dead Forest Fuels Using a Microwave Oven." Research Note INT-277. USDA Forest Service, Intermountain Forest and Range Experiment Station, Ogden.

Olson, C. M. (1980). An evaluation of the Keetch-Byram drought index as a predictor of foliar moisture content in a chaparral community. *In* "Proceedings of the Sixth Conference on Fire and Forest Meteorology," pp. 241–245. Society of American Foresters, Bethesda.

Olson, J. S. (1963). Energy storage and the balance of producers and decomposers in ecological systems. *Ecology* **44**, 322–331.

Panshin, A. J., and de Zeeuw, C. (1980). "Textbook of Wood Technology, Vol. 1," 4th ed. McGraw-Hill, New York.

Perre, P., Fohr, J. P., and Arnaud, G. (1990). A model of drying applied to softwoods: The effect of gaseous pressure below the boiling point. *In* "Drying '89" (A. S. Mujumdar and M. Roques, Eds.), pp. 91–98. Hemisphere Publishing Corporation, New York.

Philip, J. R. (1966). Plant water relations: some physical aspects. *Ann. Rev. Plant Physiol.* **17**, 245–268.

Piñol, J., Filella, I., Ogaya, R., and Peñuelas, J. (1998). Ground-based spectroradiometric estimation of live fine fuel moisture of Mediterranean plants. *Agric. For. Meteorol.* **90**, 173–186.

Plumb, O. A., Spolek, G. A., and Olmstead, B. A. (1985). Heat and mass transfer in wood during drying. *Int. J. Heat Mass Transfer* **28**, 1669–1678.

Pompe, A., and Vines, R. G. (1966). The influence of moisture on the combustion of leaves. *Aust. For.* **30**, 231–241.

Pyne, S. J. (1984). "Introduction to Wildland Fire." John Wiley, New York.

Pyne, S. J., Andrews, P. L., and Laven, R. D. (1996). "Introduction to Wildland Fire," 2nd ed. John Wiley, New York.

Riha, S. J., and Campbell, G. S. (1985). Estimating water fluxes in Douglas-fir plantations. *Can. J. For. Res.* **15**, 701–707.

Rose, C. W. (1966). "Agricultural Physics." Pergamon Press, Oxford.

Rothermel, R. C., Wilson, R. A., Jr., Morris, G. A., and Sackett, S. S. (1986). "Modeling Moisture Content of Fine Dead Wildland Fuels: Input to the BEHAVE Fire Prediction System." Research Paper INT-359. USDA Forest Service, Intermountain Research Station, Ogden.

Rothwell, R. L., Woodard, P. M., and Samran, S. (1991). The effect of soil water on aspen litter moisture content. *In* "Proceedings of the Eleventh Conference on Fire and Forest Meteorology" (P. L. Andrews and D. F. Potts, Eds.), pp. 117–123. Society of American Foresters, Bethesda.

Running, S. W. (1978). A process oriented model for live fuel moisture. *In* "Preprint Volume, Fifth Joint Conference on Fire and Forest Meteorology", pp. 24–28. Society of American Foresters, Bethesda and American Meteorological Society, Boston.

Running, S. W. (1984a). "Documentation and Preliminary Validation of H2OTRANS and DAYTRANS, Two Models for Predicting Transpiration and Water Stress in Western Coniferous Forests." Research Paper RM-252. USDA Forest Service, Rocky Mountain Forest and Range Experiment Station, Fort Collins.

Running, S. W. (1984b). Microclimate control of forest productivity: analysis by computer simulation of annual photosynthesis/transpiration balance in different environments. *Agric. For. Meteorol.* **32**, 267–288.

Rutter, A. J. (1968). Water consumption by forests. *In* "Water Deficits and Plant Growth" (T. T. Kozlowski, Ed.), Vol. 2, pp. 23–84. Academic Press, New York.

Scholl, D. G. (1976). Soil moisture flux and evaporation determined from soil hydraulic properties in a chaparral stand. *Soil Sci. Soc. Am. J.* **40**, 14–17.

Schönherr, J. (1976). Water permeability of isolated cuticular membranes: the effect of cuticular waxes on diffusion of water. *Planta* **131**, 159–164.

Schroeder, M. J., and Buck, C. C. (1970). "Fire Weather . . . A Guide for Application of Meteorological Information to Forest Fire Control Operations." Agriculture Handbook No. 360. USDA Forest Service, Washington, DC.

Shuttleworth, W. J., and Wallace, J. S. (1985). Evaporation from sparse crops—an energy combination theory. *Quart. J. Roy. Meteorol. Soc.* **111**, 839–855.

Siau, J. F. (1995). "Wood: Influence of Moisture on Physical Properties." Department of Wood Science and Forest Products, Virginia Polytechnic Institute and State University, Blacksburg.

Siau, J. F., and Avramidis, S. (1996). The surface emission coefficient of wood. *Wood Fiber Sci.* **28**, 178–185.

Simpson, W. T. (1993a). Determination and use of moisture diffusion coefficient to characterize drying of northern red oak (*Quercus rubra*). *Wood Sci. Tech.* **27**, 409–420.

Simpson, W. T. (1993b). "Specific Gravity, Moisture Content, and Density Relationship for Wood." General Technical Report FPL-GTR-76. USDA Forest Service, Forest Products Laboratory, Madison.

Skaar, C. (1988). "Wood-Water Relations." Springer-Verlag, Berlin.

Slatyer, R. O. (1967). "Plant-Water Relationships." Academic Press, New York.

Sneeuwjagt, R. J., and Peet, G. B. (1985). "Forest Fire Behaviour Tables for Western Australia." Western Australian Department of Conservation and Land Management, Perth.

Spolek, G. A., and Plumb, O. A. (1980). A numerical model of heat and mass transport in wood during drying. *In* "Drying, 1980," pp. 84–92. Hemisphere Publishing Corporation, New York.

Spolek, G. A., and Plumb, O. A. (1981). Capillary pressure in softwoods. *Wood Sci. Tech.* **15**, 189–199.

Stamm, A. J. (1946). "Passage of Liquids, Vapors and Dissolved Materials through Softwoods." Technical Bulletin No. 929, USDA, Washington, DC.

Stamm, A. J. (1960). Combined bound-water and water-vapor diffusion into Sitka spruce. *For. Prod. J.* **10**, 644–648.

Stamm, A. J. (1964). "Wood and Cellulose Science." Ronald Press, New York.

Stamm, A. J., and Harris, E. E. (1953). "Chemical Processing of Wood." Chemical Publishing Company, New York.

Stamm, A. J., and Nelson, R. M., Jr. (1961). Comparison between measured and theoretical drying diffusion coefficients for southern pine. *For. Prod. J.* **11**, 536–543.

Stocks, B. J. (1970). "Moisture in the Forest Floor—its Distribution and Movement." Publication No. 1271. Department of Fisheries and Forestry, Canadian Forestry Service, Ottawa.

Susott, R. A. (1980). Thermal behavior of conifer needle extractives. *For. Sci.* **26**, 347–360.

Susott, R. A. (1982). Characterization of the thermal properties of forest fuels by combustible gas analysis. *For. Sci.* **28**, 404–420.

Tanner, C. B. (1968). Evaporation of water from plants and soil. *In* "Water Deficits and Plant Growth" (T. T. Kozlowski, Ed.), pp. 73–106. Academic Press, New York.

Tourula, T., and Heikinheimo, M. (1998). Modelling evapotranspiration from a barley field over the growing season. *Agric. For. Meteorol.* **91**, 237–250.

Tunstall, B. (1991). Live fuel water content. *In* "Proceedings, Conference on Bushfire Modelling and Fire Danger Rating Systems" pp. 127–136. CSIRO Division of Forestry, Yarralumla.

Urqhart, A. R. (1960). Sorption isotherms. *In* "Moisture in Textiles" (J. W. S. Hearle and R. H. Peters, Eds.), pp. 14–32. Interscience, New York.

Van Wagner, C. E. (1969a). Drying rates of some fine forest fuels. *Fire Contr. Notes* **30**, 5, 7, 12.

Van Wagner, C. E. (1969b). "Combined Effect of Sun and Wind on Surface Temperature of Litter." Information Report PS-X-10. Canadian Forest Service, Petawawa Forest Experiment Station, Chalk River.

Van Wagner, C. E. (1972a). Duff consumption by fire in eastern pine stands. *Can. J. For. Res.* **2**, 34–39.

Van Wagner, C. E. (1972b). "Equilibrium Moisture Contents of Some Fine Forest Fuels in Eastern Canada." Information Report PS-X-36. Canadian Forest Service, Petawawa Forest Experiment Station, Chalk River.

Van Wagner, C. E. (1979). A laboratory study of weather effects on the drying rate of jack pine litter. *Can. J. For. Res.* **9**, 267–275.

Van Wagner, C. E. (1987). "Development and Structure of the Canadian Forest Fire Weather Index System." Forestry Technical Report 25. Canadian Forest Service, Ottawa.

Viney, N. R. (1991). A review of fine fuel moisture modelling. *Int. J. Wildland Fire* **1**, 215–234.

Viney, N. R. (1992a). "Modelling Fine Fuel Moisture Content." PhD dissertation, Department of Mathematics, University College, University of New South Wales, Sydney.

Viney, N. R. (1992b). Moisture diffusivity in forest fuels. *Int. J. Wildland Fire* **2**, 161–168.

Viney, N. R., and Catchpole, E. A. (1991). Estimating fuel moisture response times from field observations. *Int. J. Wildland Fire* **1**, 211–214.

Viney, N. R., and Hatton, T. J. (1989). Assessment of existing fine fuel moisture models applied to *Eucalyptus* litter. *Aust. For.* **52**, 82–93.

Viney, N. R., and Hatton, T. J. (1990). Modelling the effect of condensation on the moisture content of forest litter. *Agric. For. Meteorol.* **51**, 51–62.

Wallace, J. S., Roberts, J. M., and Sivakumar, M. V. K. (1990). The estimation of transpiration from sparse dryland millet using stomatal conductance and vegetation area indices. *Agric. For. Meteorol.* **51**, 35–49.

Waring, R. H., and Running, S. W. (1976). Water uptake, storage and transpiration by conifers: A physiological model. *In* "Water and Plant Life, Problems and Modern Approaches" (O. L. Lange, L. Kappen, and E.-D. Schulze, Eds.), pp. 189–202. Springer-Verlag, Berlin.

Wilson, R. A., Jr. (1990). "Reexamination of Rothermel's Fire Spread Equations in No-wind and No-slope Conditions." Research Paper INT-434. USDA Forest Service, Intermountain Research Station, Ogden.

Xanthopoulos, G., and Wakimoto, R. H. (1993). A time to ignition–temperature–moisture relationship for branches of three western conifers. *Can. J. For. Res.* **23**, 253–258.

Zhang, J., and Peralta, P. N. (1999). Moisture content–water potential characteristic curves for red oak and loblolly pine. *Wood Fiber* **31**, 360–369.